Inorganic Chemistry

Article

pubs.acs.org/IC

Model Studies of Methyl CoM Reductase: Methane Formation via CH_3−S Bond Cleavage of Ni(I) Tetraazacyclic Complexes Having Intramolecular Methyl Sulfide Pendants

Jun-ichi Nishigaki, Tsuyoshi Matsumoto,* and Kazuyuki Tatsumi*

Research Center for Materials Science, and Department of Chemistry, Graduate School of Science, Nagoya University, Furo-cho, Chikusa-ku, Nagoya 464-8602, Japan

Supporting Information

ABSTRACT: The Ni(I) tetraazacycles $[Ni(dmmtc)]^+$ and $[Ni(mtc)]^+$, which have methylthioethyl pendants, were synthesized as models of the reduced state of the active site of methyl coenzyme M reductase (MCR), and their structures and redox properties were elucidated (dmmtc, 1,8-dimethyl-4,11-bis{(2-methylthio)ethyl}-1,4,8,11-tetraaza-1,4,8,11-cyclotetradecane; mtc, 1,8-{bis(2-methylthio)ethyl}-1,4,8,11-tetraaza-1,4,8,11-cyclotetradecane). The intramolecular CH_3−S bond of the thioether pendant of $[Ni^I(dmmtc)](OTf)$ was cleaved in THF at 75 °C in the presence of the bulky thiol DmpSH, which acts as a proton source, and methane was formed in 31% yield and a Ni(II) thiolate complex was concomitantly obtained (Dmp = 2,6-dimesityphenyl). The CH_3−S bond cleavage of $[Ni^I(mtc)]^+$ also proceeded similarly, but under milder conditions probably due to the lower potential of the $[Ni^I(mtc)]^+$ complex. These results indicate that the robust CH_3−S bond can be homolytically cleaved by the Ni(I) center when they are properly arranged, which highlights the significance of the F430 Ni environment in the active site of the MCR protein.

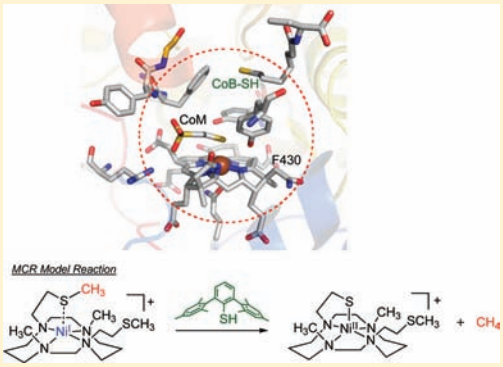

INTRODUCTION

Methyl coenzyme M reductase (MCR) is a nickel enzyme found in methanogenic archaea, which catalyzes the formation of the heterodisulfide (CoBS−SCoM) and methane from methyl CoM (MeSCoM) and *N*-7-mercaptoheptanoyl threonine phosphate (HSCoB) in the final step of methanogenesis (eq 1).[1] The active site of MCR contains a nickel corphinoid cofactor F430 (Figure 1),[2,3] and the active reduced state MCR_{red1} is suggested to contain a Ni(I) center in the F430 according to the EPR/ENDOR studies.[4] However, the mechanism of the MCR catalytic CH_3−S bond cleavage of MeSCoM has not been established.

$$\text{MeSCoM} + \text{HSCoB} \rightarrow \text{CH}_4 + \text{CoBS−SCoM}$$

$$\Delta G^{0'} = 30\,\text{kJ mol}^{-1} \quad (1)$$

Recent model studies have provided some clues to the MCR reaction mechanism.[5] Jaun and co-workers reported that photo irradiation of a Ni(II) complex of a thioether-thiolate ligand, bis(1-{2-(methylthio)ethyl}cyclohexanethiolate)nickel, in the presence of the corresponding thioether-thiol compound, 1-{2-(methylthio)ethyl}cyclohexanethiol, resulted in CH_3−S bond cleavage and gave methane and the disulfide 1,2-dithiaspiro[4,5]-decane.[5b] In this case, a key process would be generation of the Ni(I)/thiyl-radical pair via photolytic homolysis of the Ni−S(thiolate) bond, and while the results suggest an MCR catalytic pathway, the question remains how the Ni(I)/thiyl-radical pair could be generated in vivo.

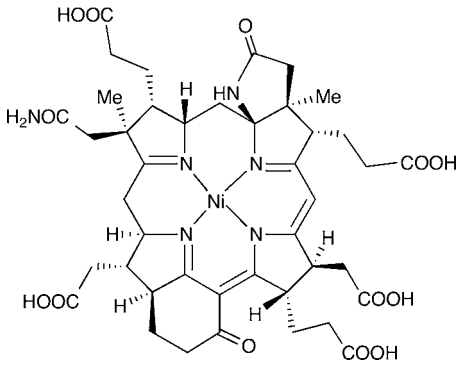

Figure 1. Cofactor F430 in MCR.

On the other hand, Siegbahn et al. have proposed a mechanism based on theoretical studies, in which the Ni(I)-F430 state is proposed to activate the CH_3−S bond of MeSCoM by interacting with tyrosine hydroxides located around the active site.[6] However, CH_3−S bond activation by Ni(I) complexes that model the active MCR_{red1} state have so far failed.[4] As reported by Ram et al., the Ni(I) tetramethylcyclam complex $[Ni(tmc)]^+$, a model for Ni(I)-F430, does not activate C−S bonds of thioethers.[5c] Jaun et al. also reported that the MCR active site became inert when it was extracted as Ni(I)-F430 pentamethyl

Received: January 4, 2012
Published: March 22, 2012

   dx.doi.org/10.1021/ic300017k | *Inorg. Chem.* 2012, 51, 5173−5187

ester, although it still cleaved sulfonium C−S bonds.[7] These results suggest that the active site environment of the protein plays a significant role. These Ni(I) complexes coordinated by four N atoms with a formal 17-electron configuration disfavor further thioether coordination,[8,9] and thus in the MCR active site, the proper positioning of MeSCoM to promote interaction with the Ni(I) center could be important. The SCoM location in the $MCR_{ox1\text{-}silent}$ state as shown in Figure 2 shows that

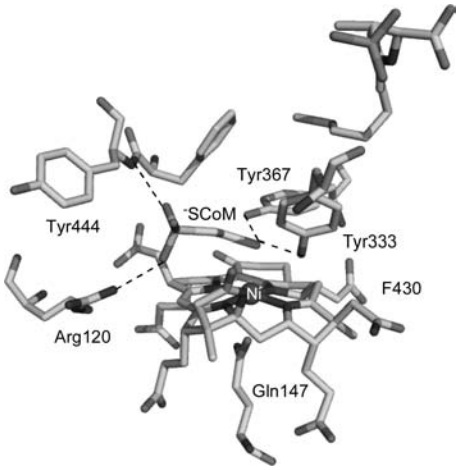

Figure 2. The MCR active site structure in the $MCR_{ox1\text{-}silent}$ state.

hydrogen bonds from protein residues hold the MeSCoM in a position favorable for interaction with the Ni(I) center, which could lead to CH_3−S bond cleavage.

In the course of our MCR model studies,[10] we have synthesized cyclam derivatives having methylthioether pendants, 1,8-dimethyl-4,11-bis{(2-methylthio)ethyl}-1,4,8,11-tetraaza-1,4,8,11-cyclotetradecane (dmmtc), and 1,8-{bis(2-methylthio)ethyl}-1,4,8,11-tetraaza-1,4,8,11-cyclotetradecane (mtc), as shown in Chart 1, to facilitate interaction between the

Chart 1

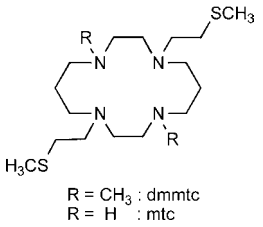

thioether sulfur and the Ni center.[11] Herein, we report the synthesis and structures of the Ni(II) and Ni(I) complexes of the dmmtc and mtc ligands. We also report that activation of the CH_3−S bond by the Ni(I) complexes models the MCR reaction.

RESULTS AND DISCUSSION

Synthesis of the Cyclam Derivatives, dmmtc and mtc. Following the report of Guilard and co-workers,[12] 1,4,8,11-tetraazatricyclo[9.3.1.1]hexadecane (**1**) was prepared from 1,4,8,11-tetraazacyclotetradecane (cyclam) and formaldehyde, and treated with 2-iodoethyl methyl sulfide. Alkylation occurred site-selectively on two trans nitrogen atoms, and compound **2** was obtained in 78% yield (Scheme 1). Compound **2** was facilely converted to dmmtc and mtc by $NaBH_4$-reduction and base hydrolysis, respectively.

Scheme 1

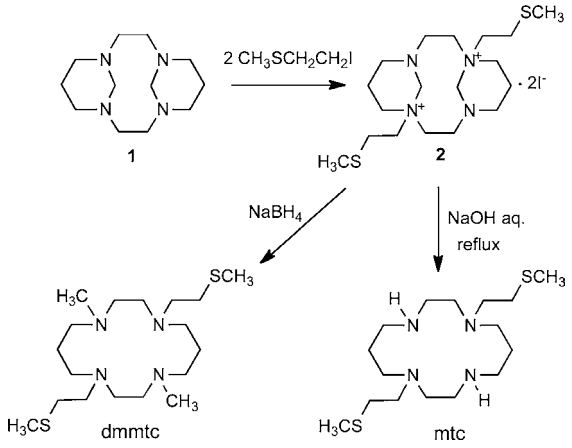

Synthesis of Ni(II) dmmtc Complexes. The dmmtc ligand dissolved in ethanol was added to an aqueous solution of $NiCl_2{\cdot}6H_2O$, which afforded [Ni(dmmtc)(Cl)](Cl) (**3**) in 67% yield as yellow-green crystals (Scheme 2). As shown by X-ray

Scheme 2

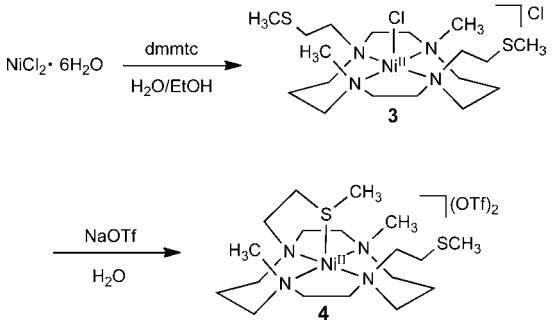

analysis, the structure features a penta-coordinate geometry around the nickel defined by the four N atoms in a basal plane and one Cl atom occupying the axial position.[13] The four alkyl groups on the nitrogen atoms of the dmmtc ligand are all on the same side of the NiN4 plane similar to the reported tetramethylcyclam analogue *RSRS*-[Ni(tmc)(Cl)]$^+$.[10a,14]

Both of the chlorides of **3** were smoothly exchanged for triflate by treatment with NaOTf in H_2O, affording [Ni(dmmtc)](OTf)$_2$ (**4**) in 76% yield as bluish green crystals. The molecular structure of **4** was also analyzed by X-ray crystallography (Figure 3), and selected bond distances and angles are listed in Table 1. The nickel assumes penta-coordination as observed for **3**, although it is a thioether sulfur of the dmmtc ligand that caps the nickel in place of a chloride. As indicated by the substantially bent N2−Ni−N4 bond (148.75(7)°) and linear N1−Ni−N3 bond (175.01(7)°), the coordination geometry of the nickel can be described either as a distorted square pyramid with the sulfur occupying the apical position or as a distorted trigonal bipyramid where N1 and N3 are at the axial positions. The Ni−S distance (2.4005(6) Å) resembles those of previously reported penta-coordinate nickel(II) thioether complexes.[7b,15]

In acetonitrile, cyclic voltammetry (CV) of **4** exhibited a single reversible couple at −1.09 V in (vs $Ag/AgNO_3$, Figure 4), which we assign to the Ni^I/Ni^{II} redox process. This potential is close to the value of *RSRS*-[Ni(tmc)]$^{2+}$ (−1.14 V),[5c] but is considerably

dx.doi.org/10.1021/ic300017k | *Inorg. Chem.* 2012, 51, 5173−5187

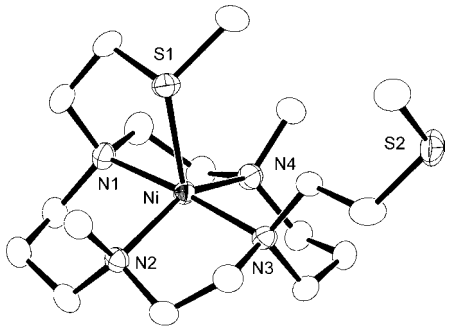

Figure 3. Molecular structure of the cation of **4** with 50% thermal ellipsoids. Hydrogen atoms are omitted for clarity.

Table 1. Selected Bond Distances (Å) and Angles (deg) for 4

	4
Ni–S1	2.4005(6)
Ni–N1	2.126(2)
Ni–N2	2.1340(19)
Ni–N3	2.131(2)
Ni–N4	2.122(2)
S1–Ni–N1	84.59(5)
S1–Ni–N2	100.15(5)
S1–Ni–N3	100.30(7)
S1–Ni–N4	110.75(5)
N1–Ni–N3	175.01(7)
N2–Ni–N4	148.75(7)

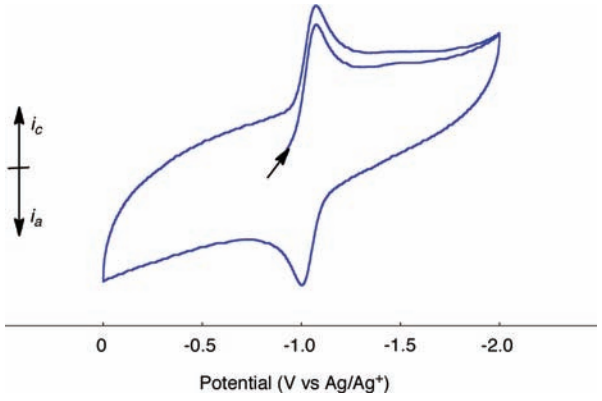

Figure 4. Cyclic voltammogram of 0.5 mM of **4** in CH_3CN at 0.2 V s^{-1} with 0.1 M $(Bu_4N)(PF_6)$ as the supporting electrolyte. Potentials are referenced to $Ag/AgNO_3$.

less negative (by ca. 0.4 V) than that of F430 pentamethyester.[16,17]

Synthesis of Ni(II) mtc Complexes. Similar to the synthesis of **3**, the mtc ligand was allowed to react with $NiCl_2{\cdot}6H_2O$ in ethanol/H_2O. The crude product was found to contain two complexes, $[Ni^{II}(mtc)(Cl)](Cl)$ (**5a**) and $[Ni^{II}(mtc)(OH_2)_2](Cl)_2$ (**5b**) (Scheme 3), which were separated by extraction with H_2O. Thus, complex **5b**, insoluble in H_2O, was isolated in 16% yield as a light purple powder, while **5a** was obtained in 63% yield as a light blue powder via evacuation of the filtrate and extraction with $CHCl_3$. X-ray crystallography revealed hexa-coordinate structures for the nickels of both **5a** and **5b** (Figure 5, Tables 2 and 3). In complex **5a**, a thioether sulfur and a chloride coordinate in cis-positions, and the mtc ligand coordinates in a *fac–mer* fashion, whereas the four nitrogens of mtc in **5b** are coplanar with a *mer–mer*

Scheme 3

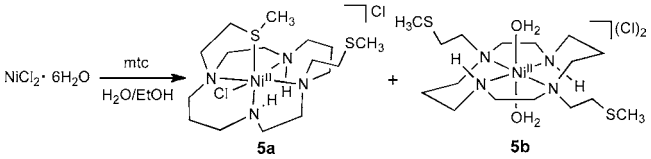

configuration, and two H_2O molecules are bound to the axial positions.[19]

Treatment of **5a** or **5b** with NaOTf in H_2O gave the corresponding triflate complexes **6a** and **6b**, and their structures were also confirmed by X-ray analysis. While complex **6a** retains the hexa-coordinate geometry by incorporating a second thioether sulfur instead of the removed chloride, complex **6b** assumes a tetra-coordinate square planar geometry with dissociation of the H_2O molecules.[20] The different geometry of **6a** and **6b** was evident from the color, light purple for **6a** and orange for **6b**.

The triflate complexes **6a** and **6b** were further converted to the borate complexes **7a** and **7b**, respectively, as shown in Scheme 4. On the basis of its purple color, we assume that **7a** has an octahedral geometry like that of **6a**. However, X-ray analysis was not performed. In contrast to the orange **6b**, simple anion exchange to produce **7b** leads to a purple product, indicating a hexa-coordinate complex. X-ray structural analysis confirms that the two thioethers have bound to the nickel producing a pseudo octahedral complex. Because the counteranions do not interact with the respective nickel cations significantly in either **6b** or **7b**, the geometrical difference found for **6b** and **7b** must be attributable to crystal packing, indicating that the thermodynamic stabilities of the two geometries must be only slightly different.

To investigate the redox properties of **6a** and **7b**, cyclic voltammograms were generated. In THF, complex **6a** shows a Ni^{II}/Ni^{I} redox couple at $E_{1/2} = -1.36$ V (vs Ag/Ag^+) as shown in Figure 6b. Complex **7b** also exhibits a similar reversible Ni^{I}/Ni^{II} redox couple at −1.35 V. These $E_{1/2}$ values are ca. 0.4 V more negative as compared to that of the penta-coordinate dmmtc complex **4**.[21] While the shape of the CV plot of **7b** did not noticeably change with scan rate between 0.01 and 0.2 V s^{-1}, that of **6a** was considerably different at a slower scan rate. At a sweep rate of 0.01 V s^{-1}, the anodic current of the Ni^{II}/Ni^{I} couple became significantly smaller, and an additional irreversible anodic wave emerged at +0.17 V (Figure 6a), indicating further reaction of the generated Ni(I) species. Because this oxidation potential of +0.17 V compares well with the value reported for the related N_4-coordinated Ni(II) thiolate complex $[L^8py_2Ni(STol)](BPh_4)$ (L^8py_2 = 1,5-bis(2-pyridylmethyl)-1,5-diazacyclooctane),[22] we conclude that the Ni(I) species generated by reduction of **6a** has been converted into Ni(II) thiolate complex via reductive cleavage of the CH_3–S bond.

Synthesis of Monovalent Nickel Complexes [Ni(dmmtc)](X) (8, X = OTf; 9, X = BAr^F_4). Noting the CV data for **4** and choosing an appropriate reducing agent, treatment of **4** with 0.3% Na/Hg in THF/CH_3CN smoothly generated the corresponding nickel(I) complex [Ni(dmmtc)](OTf) (**8**) in 72% yield as blue plate crystals (Scheme 5). Complex **8** was converted to the borate analogue $[Ni(dmmtc)](BAr^F_4)$ (**9**) by ion exchange with $NaBAr^F_4$ in Et_2O, which was isolated in 70% yield. However, the crystals were yellow, indicating different coordination geometries of **8** and **9** in the crystals. The molecular structures were confirmed by X-ray analysis, showing that the

dx.doi.org/10.1021/ic300017k | Inorg. Chem. 2012, 51, 5173–5187

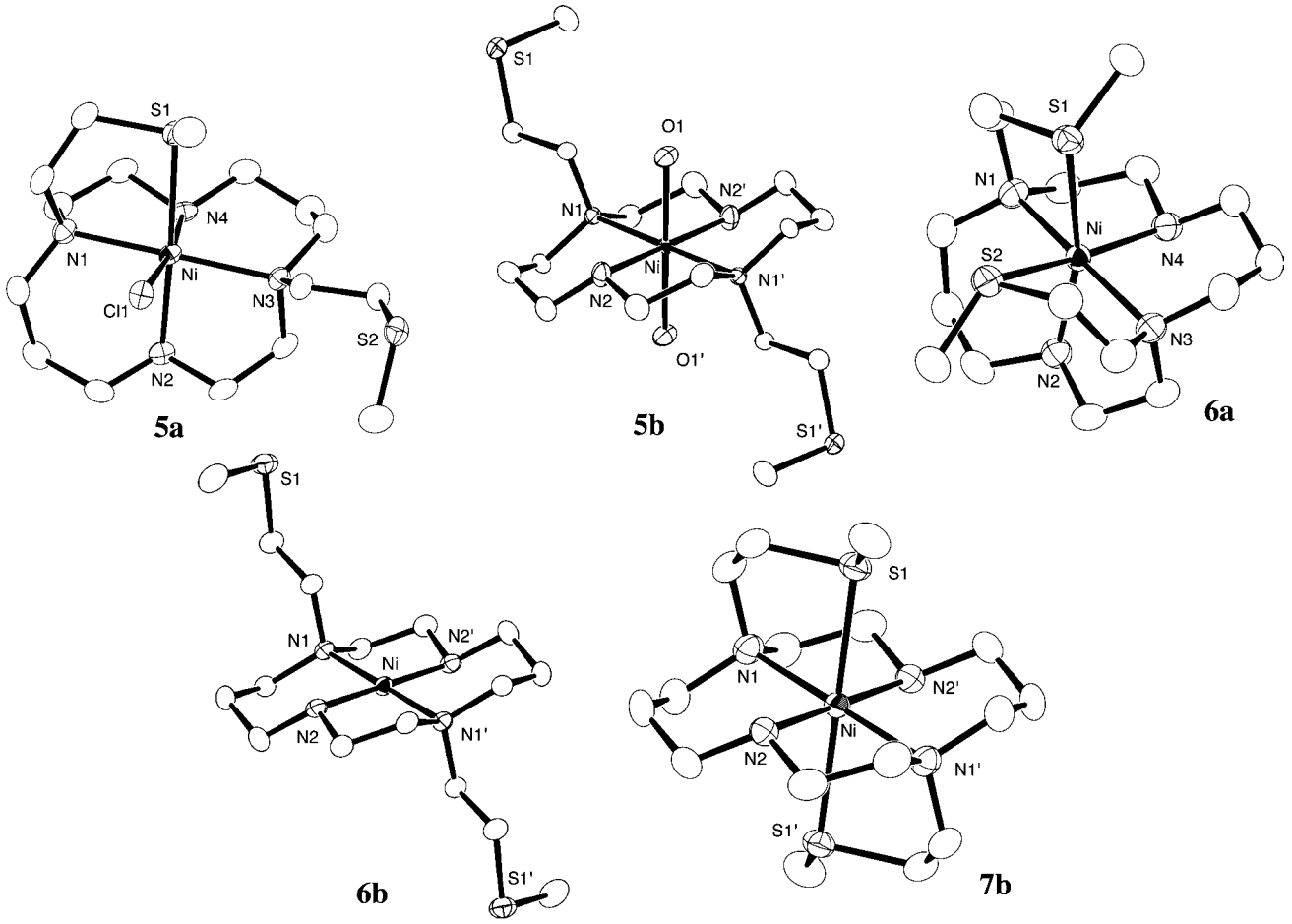

Figure 5. Molecular structures of the cations of **5a,b**, **6a,b**, and **7b** with 50% thermal ellipsoids. Hydrogen atoms are omitted for clarity.

Table 2. Selected Bond Lengths (Å) and Angles (deg) for 5a, 6a

	5a	6a
Ni–S1	2.4374(4)	2.5614(13)
Ni–L1[a]	2.5299(6)	2.6187(13)
Ni–N1	2.1582(13)	2.168(4)
Ni–N2	2.0846(17)	2.069(4)
Ni–N3	2.1982(13)	2.169(4)
Ni–N4	2.1248(13)	2.072(4)
S1–Ni–L1[a]	91.494(17)	70.47(4)
S1–Ni–N1	89.68(3)	83.24(10)
S1–Ni–N2	89.43(3)	164.73(11)
S1–Ni–N3	96.19(3)	103.37(10)
S1–Ni–N4	172.39(4)	98.95(10)
L1–Ni–N1[a]	83.89(4)	104.29(10)
L1–Ni–N2[a]	177.30(3)	97.92(11)
L1–Ni–N3[a]	98.65(4)	82.82(10)
L1–Ni–N4[a]	85.15(4)	165.19(11)
N1–Ni–N3	173.52(5)	171.73(14)
N2–Ni–N4	93.63(6)	94.16(14)

[a]L1 = Cl1 (**5a**), S2 (**6a**).

Table 3. Selected Bond Lengths (Å) and Angles (deg) for 5b, 6b, and 7b

	5b	6b	7b
Ni–L2[a]	2.135(3)		2.5460(8)
Ni–N1	2.167(2)	1.9710(19)	2.127(2)
Ni–N2	2.042(3)	1.9334(17)	2.062(3)
L2–Ni–N1[a]	92.55(10)		80.71(8)
L2–Ni–N2[a]	86.81(13)		91.89(8)
L2–Ni–N3[a]	87.45(10)		99.29(8)
L2–Ni–N4[a]	93.19(13)		88.11(8)

[a]L2 = O1 (**5b**), S2 (**7b**).

nickels of **8** and **9** assume tetra- and penta-coordination, respectively (vide infra). However, THF solutions of **8** and **9** show the same green color. Their UV–vis spectra exhibit two common absorptions, a CT band at 333 nm (ε = 3600 cm^{-1} M^{-1}) and a d–d* band at 717 nm (ε = 20 cm^{-1} M^{-1}), which compare well with those of *RSRS*-[Ni(tmc)](OTf) that includes a tetra-coordinate geometry in solution.[5c,23] Probably, the penta-coordinate structure found for the crystal of **9** would be thermodynamically less favored due to the coordinative saturation of the d^9-electron configuration of the monovalent nickel center.[8]

Molecular Structures of 8 and 9. The structures of **8** and **9** are shown in Figure 7, and their metric parameters are listed in Table 4. Complex **8** contains a tetra-coordinate nickel sitting in a nearly square planar geometry with a tetrahedral distortion with N1 and N3 above the mean plane and N2 and N4 below it. This structural feature is also found in the reported Ni(I) complex *RSRS*-[Ni(tmc)](OTf).[24] Further structural details of **8** will not be discussed because the dmmtc ligand is fully disordered around the axis vertically penetrating the nickel.

The borate analogue **9** contains a nickel structurally different from that of **8**. The nickel center is coordinated by a thioether sulfur in addition to the four nitrogens, forming a distorted square pyramidal geometry. Although it appears similar to the

dx.doi.org/10.1021/ic300017k | *Inorg. Chem.* 2012, 51, 5173–5187

Scheme 4

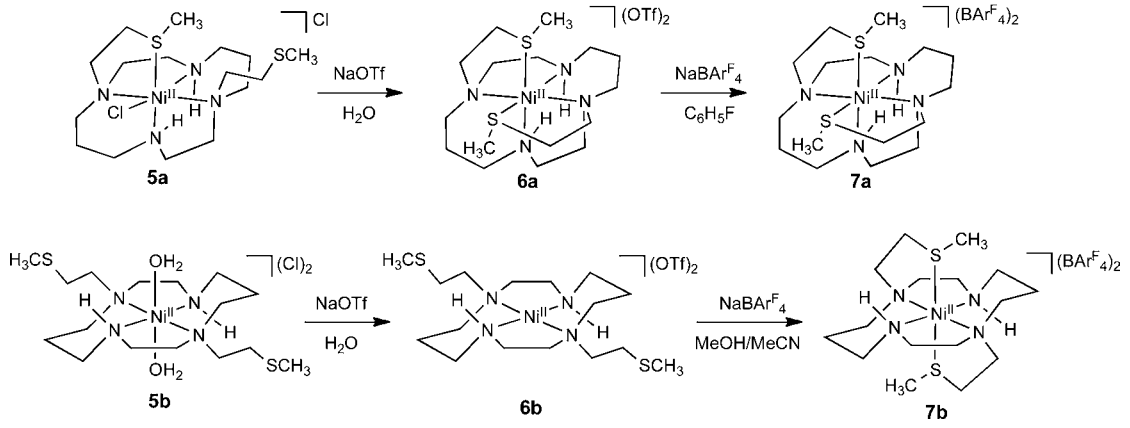

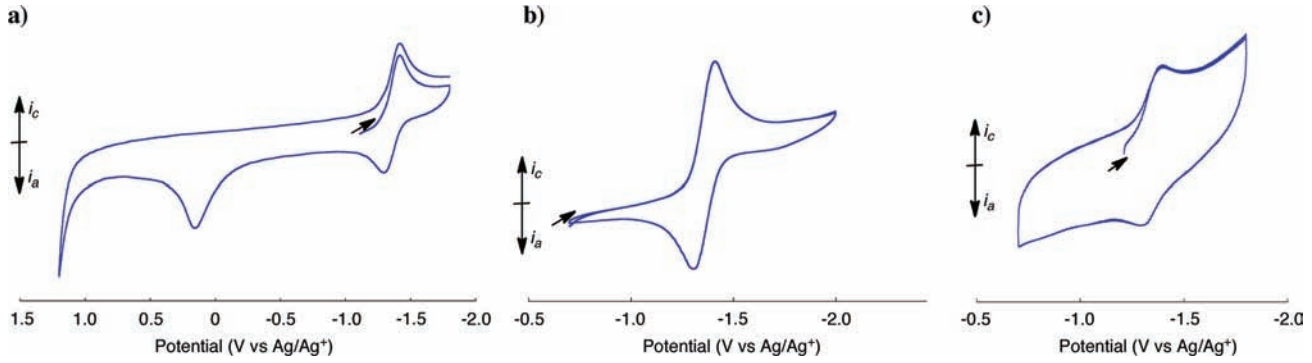

Figure 6. Cyclic voltammogram of 0.5 mM of **6a** in THF with scan rates of (a) 0.01 V s^{-1}, (b) 0.2 V s^{-1}, and (c) 0.5 mM of **7b** in THF with a scan rate of 0.1 V s^{-1}. Potentials are referenced to $Ag/AgNO_3$.

Scheme 5

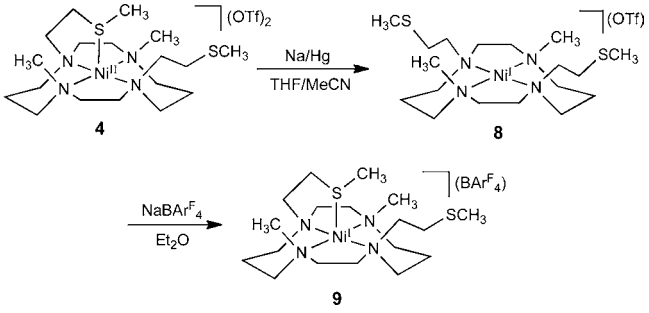

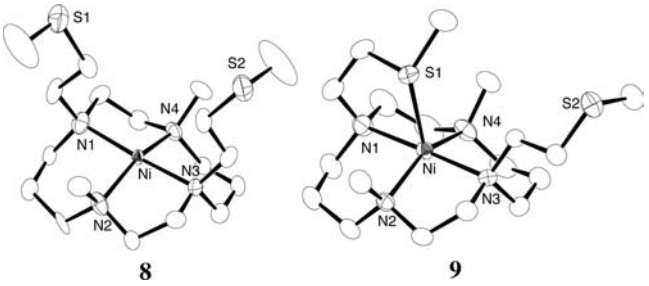

Figure 7. Molecular structures of the cations of **8** and **9** with 50% thermal ellipsoids. For **8**, one component of the 2-fold disordered ligand as well as hydrogen atoms are omitted for clarity.

related Ni(II) complex **4**, the Ni−S bond is reasonably elongated by 0.12 Å due to the larger coordination sphere of the reduced nickel. The nickel also approaches to the basal N_4 plane for **9** as indicated by the wider N1−Ni−N3 and N2−Ni−N4 bonds (178.32(11)° and 151.24(11)°) than the corresponding bond angles of **4**, respectively.

Table 4. Selected Bond Lengths (Å) and Angles (deg) in 8, 9, and 10a,b

	8	9	10a	10b
Ni−S1		2.5243(9)	3.1576(7)	
Ni−N1	2.125(7)	2.150(2)	2.1223(5)	2.118(4)
Ni−N2	2.084(6)	2.108(2)	2.0263(5)	2.029(5)
Ni−N3	2.123(7)	2.176(2)	2.1041(6)	(2.118(4))
Ni−N4	2.076(5)	2.116(2)	2.0235(6)	(2.029(5))
S1−Ni−N1		84.14(8)	77.502(14)	
S1−Ni−N2		100.96(7)	96.70(2)	
S1−Ni−N3		99.52(7)	93.441(13)	
S1−Ni−N4		107.50(8)	121.017(8)	
N1−Ni−N3	174.6(3)	178.32(11)	170.296(3)	180
N2−Ni−N4	157.3(3)	151.24(11)	155.249(7)	180

Synthesis of $[Ni^{I}(mtc)]X$ (X = OTf, BAr^{F}_{4}). Following the successful synthesis of the dmmtc complexes, the synthesis of mtc complexes of Ni(I) was similarly attempted via reduction of the corresponding Ni(II) complexes. When complex **7a** was treated with Na/Hg at room temperature in Et_2O/THF (10:1), the solution immediately became green as was also observed for the reduction of **4**. However, the green solution evolved into reddish brown within a few minutes, indicating thermal instability of the reduced species as was suggested by the CV data in Figure 6a (vide supra). To trap the transient species, reduction and successive crystallization were performed at −40 °C, which gave the Ni(I) mtc complex **10a** as yellow green crystals in 16% yield

dx.doi.org/10.1021/ic300017k | Inorg. Chem. 2012, 51, 5173−5187

Scheme 6

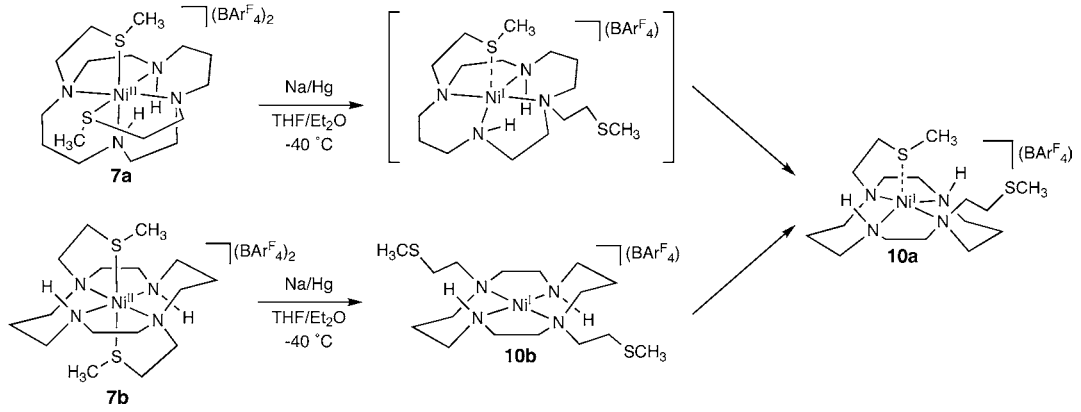

(Scheme 6). A similar reduction of the trans stereoisomer **7b** also gave **10a**, but with a higher yield of 51%. Partial inversion of the mtc nitrogen atoms occurs in the course of both reductions. The reduction of **7b** occasionally afforded a trace amount of **10b**, which has the same stereo configuration as **7b**. Thus, reduction of **7b** first affords the intermediate Ni(I) species **10b** that conserves the nitrogen stereochemistry as shown in Scheme 6. Gradual isomerization to the thermodynamic product **10a** follows.[8] The reduction of **7a** should follow a similar pathway, although the intermediate has not been observed.

We also examined the reduction of the triflate complexes **6a** and **6b**. Although the triflate salt [Ni(mtc)]OTf (**11**) has not been isolated, the reduction seems to have proceeded similarly, because anion exchange with $NaBAr^F_4$ afforded **10a** although the yield was low.

The molecular structures of **10a** and **10b** were established by X-ray analysis (Figures 8, 9 and Table 4).[25] In complex **10a**,

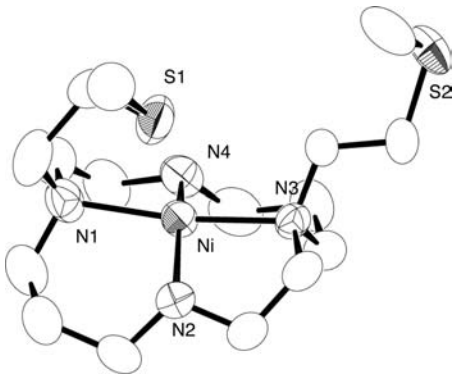

Figure 8. Molecular structure of the cation of **10a** with 50% thermal ellipsoids. Disordered atoms and hydrogen atoms are omitted for clarity.

the substituents on the nitrogen atoms are all cofacial up, and one thioether sulfur is located above the nickel. Although this geometry appears similar to that of Ni(I) dmmtc complex **9**, the Ni–S distance of 3.1576(7) Å is considerably longer than that of **9** (2.5243(9) Å) and is nearly as long as the sum of their van der Waals radii (3.43 Å).[26] In addition, the nickel exhibits a tetrahedral distortion as observed for **8**, which displaces N1 and N3 from the coordination plane toward S1, while N2 and N4 are displaced toward the opposite side of the coordination plane. We concluded that any Ni–S interaction is insignificant. Complex **10b** also contains a tetra-coordinate nickel center, and irrespective of the reduced Ni(I) oxidation state, the geometry

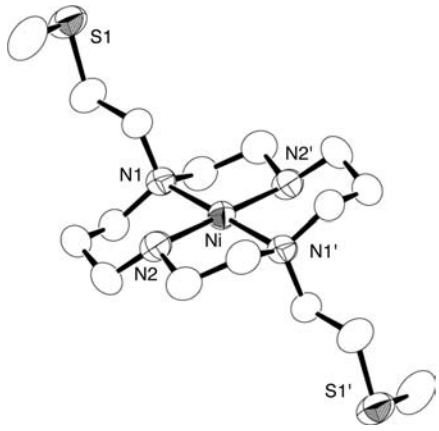

Figure 9. Molecular structures of the cation of **10b** with 50% thermal ellipsoids. Hydrogen atoms are omitted for clarity.

of **10b** is square planar as was the case for the related Ni(II) complex **6b**, although the Ni–N distances are reasonably longer by 0.05–0.19 Å.

EPR Spectra. The EPR spectra of **8**, **9**, and **10a** were recorded in the solid state Figure 10. Complex **8** exhibited an axial signal with $g_{\|} = 2.32$ and $g_{\perp} = 2.07$ as shown in Figure 10a, which resembles that of the square planar Ni(I) complex $[Ni(tmc)]^+$.[27] Interestingly, the spectra of **9** and **10a** also show similar axial EPR signals with $g_{\|} = 2.35$, $g_{\perp} = 2.10$ for **9** and $g_{\|} = 2.30$, $g_{\perp} = 2.08$ for **10a**, and the data are distinct from the spectra of the penta-coordinated Ni(I) cyclam complex $[Ni(cyclam)(CO)]^+$ ($g_1 = 2.196$, $g_2 = 2.137$, $g_3 = 2.017$).[28] The results indicate that in both **9** and **10a** the thioether sulfur coordination along the *z*-axis is weak as suggested by the X-ray results and is too weak to effect the unpaired electron localized in the nearly orthogonal $d_{x^2-y^2}$ orbital.

Intramolecular CH_3–S Bond Activation by 8. While the Ni(I) complex **8** was stable in the solid state, it was found to degrade slowly in solutions via C–S bond activation. When complex **8** was warmed in THF to 75 °C for 4 days in a sealed flask, methane (6%), ethane (23%), and ethylene (3%) were detected by gas chromatography.[29] Because the Ni(II)–thiolate complex **12** was concomitantly obtained from the resultant solution as yellowish green crystals in 19% yield, the CH_3–S bond in a pendant arm of **8** must have been cleaved in the course of the reaction (Scheme 7).[30] In this reaction, the oxidized nickel(II) complex **4** and its stereoisomer **4′** were also obtained as blue green and light blue crystals, respectively.[31] Two additional

dx.doi.org/10.1021/ic300017k | Inorg. Chem. 2012, 51, 5173–5187

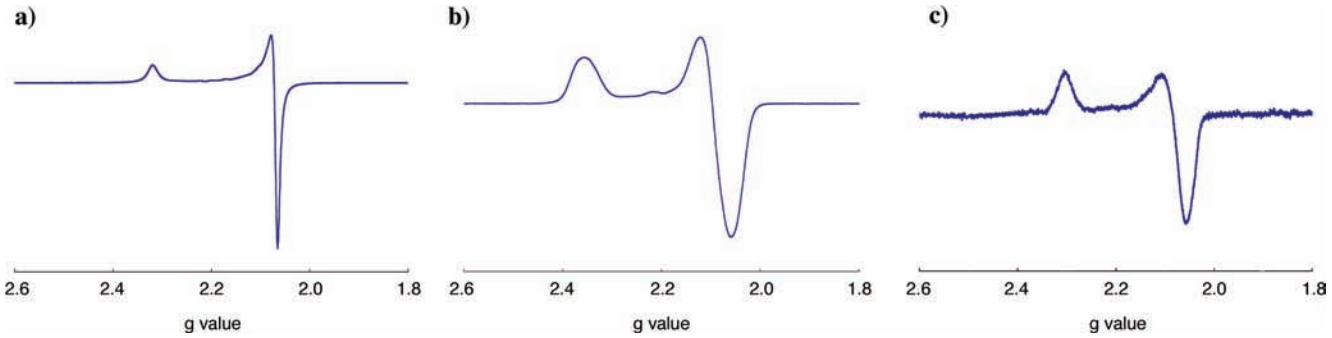

Figure 10. X-Band solid-state EPR spectra of (a) **8** and (b) **9** recorded at 8 K, and (c) **10a** recorded at 190 K. Spectrometer settings: microwave frequency, 9.37 GHz; microwave power, 1 mW; modulation frequency, 100 kHz; modulation amplitude, 5 G.

Scheme 7

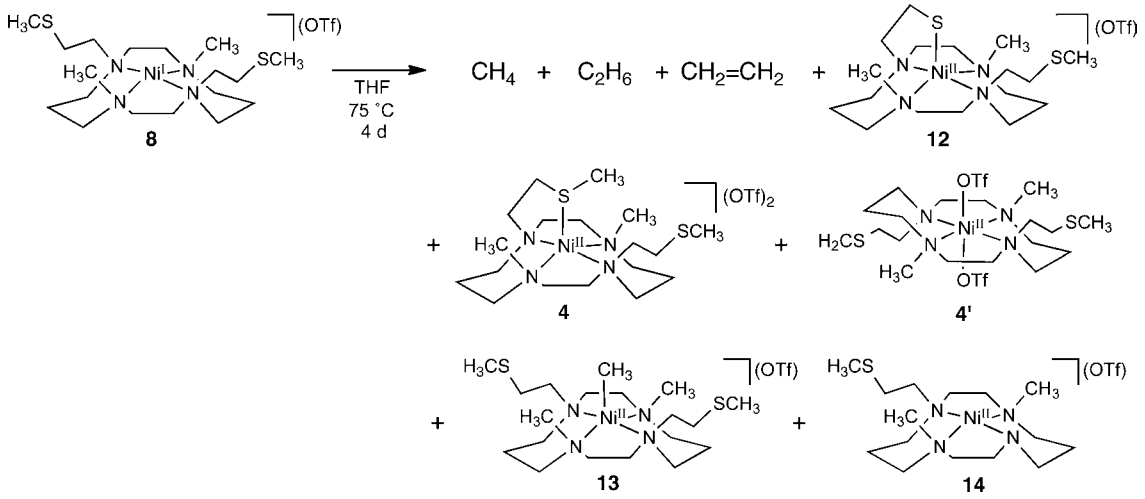

Ni(II) complexes, the Ni(II)−CH_3 complex $[Ni(dmmtc)(CH_3)]^+$ (**13**) and the Ni(II) amido complex **14** that has lost one thioether pendant, were observed in the ESI-TOF-MS. Although there have been several reports of C−S bond cleavage mediated by transient Ni(I) species that were generated in situ and have not been isolated or fully characterized,[5a,b,32] this reaction would serve as a rare example of C−S bond cleavage mediated by an isolated well-characterized Ni(I) complex.

As a coenzyme B model, we also examined the similar reaction of **8** in the presence of added thiol. Sterically less demanding thiols such as *p*-toluenethiol were directly reduced by the Ni(I) center to afford H_2 and the nickel(II) thiolate.[33] However, the very bulky arenethiol DmpSH (Dmp = 2,6-dimesitylphenyl)[34] did not react at room temperature, and thus in the presence of 5 equiv of DmpSH, complex **8** was allowed to warm to 75 °C in THF (Table 5). The thiol addition did not cause significant acceleration of the reaction, but GC analysis indicated that the methane yield was increased up to 31% while ethane formation was almost completely suppressed. The nickel products were almost identical to those from the run in the absence of the thiol; the thiolate complex **12** was isolated in 21% yield, and ESI-TOF-MS showed the formation of the Ni(II) complexes **4** and **4′**, the methyl complex **13**, and the amido complex **14**. In addition to these products, $DmpSCH_3$ was obtained in 12% yield.[35]

Table 5. Hydrocarbon Yields from the Ni(I) Complex 8

additives	CH_4 (%)	C_2H_6 (%)	C_2H_4 (%)
	6	23	3
5 equiv of DmpSH	31	trace	3

The molecular structure of **12** was confirmed by X-ray analysis as shown in Figure 11. The nickel assumes a penta-coordination, resembling that of **4**. However, the Ni−S1 bond is 0.1 Å shorter (Table 6).[36]

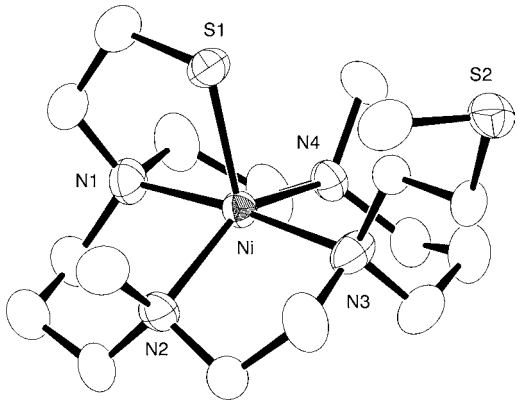

Figure 11. Molecular structure of the cation of **12** with 50% thermal ellipsoids. Hydrogen atoms are omitted for clarity.

Mechanism: Reaction of 8. To corroborate the source of the methyl fragment in the products, we prepared the bis *S*-trideuteriomethyl analogue of the dmmtc ligand dmmtc-d_6

dx.doi.org/10.1021/ic300017k | *Inorg. Chem.* 2012, 51, 5173−5187

Table 6. Selected Bond Lengths (Å) and Angles (deg) for 12

	12
Ni−S1	2.2954(13)
Ni−N1	2.133(4)
Ni−N2	2.153(3)
Ni−N3	2.161(3)
Ni−N4	2.132(3)
S1−Ni−N1	87.81(11)
S1−Ni−N2	106.37(10)
S1−Ni−N3	98.27(10)
S1−Ni−N4	106.15(10)
N1−Ni−N3	173.93(14)
N2−Ni−N4	147.32(14)

and synthesized the Ni(I) complex [Ni(dmmtc-d_6)](OTf) (**8**-d_6). When the reaction of **8**-d_6 was similarly examined in the presence of DmpSH, formation of CD_3H and C_2D_6 was observed by GC−MS, indicating that the methane and the ethane resulted from the methylthio portions of the dmmtc pendants. In addition, the CD_3-coordinated Ni(II) complex $[Ni(dmmtc\text{-}d_6)(CD_3)]^+$ was observed by ESI-TOF-MS analysis, and the deuterated methylthioether $DmpSCD_3$ was obtained. On the other hand, the ethylene was not deuterated. The formation of the amido complex **14** requires the loss of a $CH_2CH_2SCH_3$ group, which must be the source of the ethylene.

On the basis of these results, a proposed reaction mechanism is depicted in Scheme 8. Activation of the CH_3−S bond,

Scheme 8

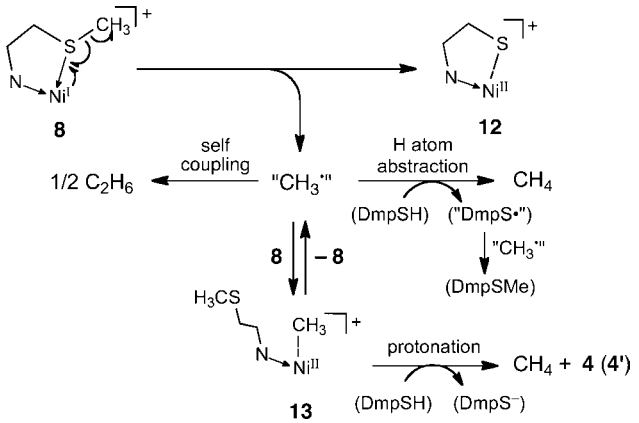

achieved by the intramolecular interaction of the thioether sulfur and the Ni(I) center, results in homolytic cleavage of the CH_3−S bond.[37] The "CH_3" radical would give methane via hydrogen abstraction and ethane by self-coupling. It may also add to another nickel(I) complex **8** to give the nickel(II) methyl complex **13**, although it would release "CH_3" radical as suggested in the thermal reaction of the related Ni(II) methyl complex [Ni(tmc)CH_3](OTf).[38]

In the presence of the thiol DmpSH, the formation of methane was enhanced, while that of ethane was largely suppressed. The result indicates that the thiol serves as a hydrogen donor.

On the other hand, ethylene, which derives from the methylthioethyl pendants, can be formed via activation of the other C−S bond of the thioether, the CH_2−SCH_3 bond. As shown in Scheme 9, homolysis of the C−S bond would generate a nickel(II) thiolate and a radical Ni^{II}(SMe)−N−CH_2−CH_2·, which would be further converted to ethylene, Ni(II) amide **14**, and a CH_3S· fragment.

Scheme 9

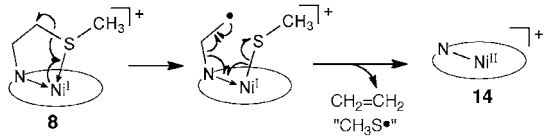

CH_3−S Bond Activation of [Ni^I(mtc)]X (X = OTf, BAr^F_4). The negatively shifted redox potential of **10a** as compared to the dmmtc complex **8** suggests a higher driving force and thus a faster reaction (Scheme 10). Indeed, the reduction of **10a** occurs at a lower temperature and in hours rather than days. When **10a** was stirred for 12 h at room temperature in THF, formation of methane (18%), ethane (trace), and ethylene (2%) was observed by GC analysis. The ESI-TOF-MS spectra showed a signal at m/z = 391.1 attributable to the Ni(II) thiolate complex **15**. The mass spectra also exhibited another strong signal at m/z = 405.1, which is 1 mass-unit smaller than that of **10a**. Probably the NH proton of the mtc ligand is consumed as a hydrogen source for methane formation, and the Ni(II) amide complex **16** would also form. Although the X-ray crystallographic analysis of **15** and **16** has not been achieved, their structures were confirmed for their triflate analogues (vide infra).

It is notable that the methane yield was considerably higher when the Ni(I) species were prepared in situ from **7a** at −40 °C in THF by treatment with Na/Hg and successive removal of the reductant. When the solution was warmed to room temperature and stirred for 6 h, the methane yield was increased to 34%, while the yields of ethane and ethylene did not vary significantly. Probably the reduction of **7a** first afforded the Ni(I) complex with retention of the ligand conformation as shown in Scheme 6, in which the CH_3−S bond could be cleaved more facilely than the case of **10a**, although the reason for the higher reactivity is unclear.

We have also carried out the same reaction with the triflate analogue **6a** (Scheme 11). Because the corresponding Ni(I) complex has not been isolated as described above, complex **6a** was similarly reduced in situ over Na/Hg in THF, and the solution was stirred for 6 h at room temperature. The GC analysis showed the formation of methane in 30% yield and ethylene in 2% yield, while ethane was not detected. In the MS spectra, the Ni(II)−thiolate complex **17** and the Ni(II)−amide complex **18**, the triflate analogues of **15** and **16**, respectively, were observed. Recrystallization of the crude mixture afforded **17** in 9% yield as green crystals and **18** in 5% yield as deep blue crystals,[30] and their structures were confirmed by X-ray crystallography.

The molecular structures of **17** and **18** are shown in Figures 12 and 13, and selected bond distances and angles are summarized in Table 7. In the thiolate complex **17**, the nitrogen stereo configuration of the mtc ligand matches that of the starting complex **6a**. However, the thioether sulfur does not coordinate to the nickel in **17** probably due to the strong coordination of the thiolate, and thus the nickel of **17** becomes trigonal bipyramidal. The axial Ni−N distances (2.1513(17) and 2.2013(18) Å) are elongated from those in equatorial positions of 2.0683(17) and 2.0780(16) Å.

The amide complex **18** in Figure 13 contains a square planar nickel coordinated by four N atoms of the mtc ligand, while the thioethers do not interact with the nickel center. The Ni−N4 distance of 1.8747(19) Å is significantly shorter than the other

dx.doi.org/10.1021/ic300017k | Inorg. Chem. 2012, 51, 5173−5187

Scheme 10

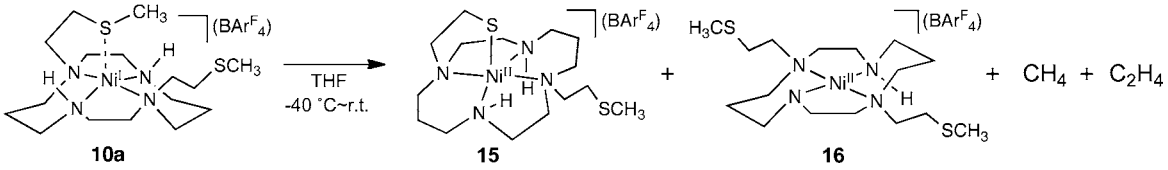

Scheme 11

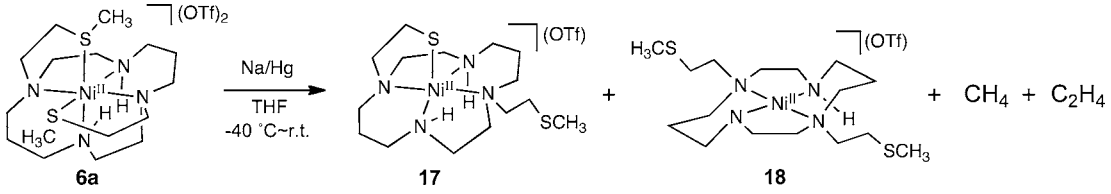

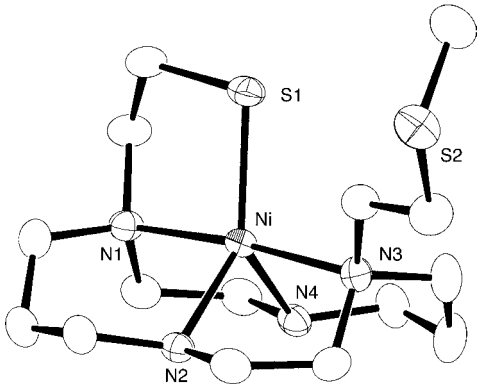

Figure 12. Molecular structure of the cation of **17** with 50% thermal ellipsoids. Hydrogen atoms are omitted for clarity.

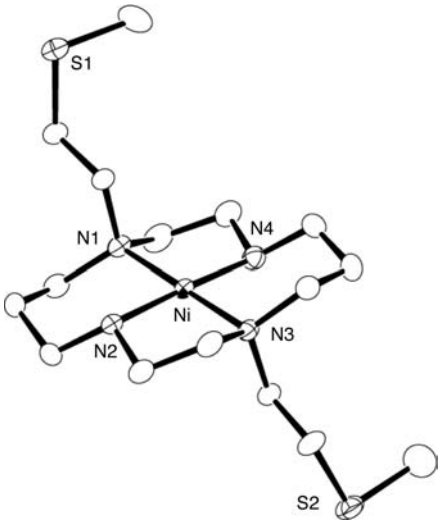

Figure 13. Molecular structure of the cation of **18** with 50% thermal ellipsoids. Hydrogen atoms are omitted for clarity.

Ni–N distances by 0.09 Å, clearly indicating that N2 is coordinating as an amide.

SUMMARY

As models of the MCR active site in the reduced state, Ni(I) complexes coordinated by cyclam derivatives that carry methylthioether pendants have been synthesized and investigated for their reactivity. A significant finding is that the robust CH_3–S bond was cleaved by nickel(I) when the thioether sulfur was arranged close to the nickel center. The protein residues around the MCR active site seem to play a crucial role to arrange the substrates properly. As the Ni(I) mtc complex cleaved the CH_3–S bond more facilely as compared to that of the dmmtc complex, the Ni(I)/Ni(II) potential would be important for efficient catalysis. Another important finding is that the CH_3–S bond cleavage promoted by the nickel(I) occurs homolytically to afford a nickel(II) thiolate and a "CH_3" radical. These result supports the suggestion that the Ni(I) state is a plausible active state in MCR catalysis.

Table 7. Selected Bond Lengths (Å) and Angles (deg) for 17 and 18

	17	18
Ni–S1	2.2343(5)	
Ni–N1	2.1513(17)	1.9685(12)
Ni–N2	2.0683(17)	1.9680(18)
Ni–N3	2.2013(18)	1.9642(12)
Ni–N4	2.0780(16)	1.8747(19)
S1–Ni–N1	88.45(4)	
S1–Ni–N2	134.93(4)	
S1–Ni–N3	96.94(4)	
S1–Ni–N4	127.13(5)	
N1–Ni–N3	174.60(6)	179.54(7)
N2–Ni–N4	97.74(6)	177.71(6)

EXPERIMENTAL SECTION

General Procedures. All reactions and manipulations were conducted under an inert atmosphere of dry nitrogen by employing standard Schlenk techniques or a glovebox under a nitrogen atmosphere. Pentane, hexane, ether, THF, and acetonitrile were degassed and purified by the method of Grubbs, where the solvents were passed over columns of activated alumina and supported copper catalyst supplied by Hansen & Co. Ltd. Fluorobenzene was distilled from sodium benzophenone ketyl. Methanol, ethanol, and nitromethane were purchased and used without further purification. C_6D_6 was dried over sodium and distilled prior to use. ^{1}H NMR (600 MHz) and ^{13}C{^{1}H} NMR (243 MHz) spectra were recorded on a JEOL ECA-600. The signals were referenced to the residual proton peak of the deuterated solvents. UV–vis spectra were recorded in 10 mm quartz glass cells on a JASCO V560 or SHIMAZU UV3150 spectrometer. Electrospray ionization time-of-flight mass spectrometry (ESI-TOF-MS) spectra were obtained from a Micromass LCT TOF-MS spectrometer. Elemental analyses were recorded on a LECO-CHNS-932 elemental analyzer where the crystalline samples were sealed in silver capsules under nitrogen. EPR spectra were collected on

dx.doi.org/10.1021/ic300017k | Inorg. Chem. 2012, 51, 5173–5187

a Bruker EMX-plus spectrometer at X-band frequencies with a liquid helium cryostat. Nickel halides, nickel triflate, and the other common reagents were purchased and used without further purification. 1,4,8,11-Tetraazatricyclo[9.3.1.1]hexadecane,[12] 2-iodoethyl methyl sulfide,[39] and DmpSH[34] were prepared according to literature procedures.

Materials. *1,8-Bis(2-methylthioethyl)-4,11-diazoniatricyclo-[9.3.1.1]hexadecane Diiodide (**2**).* Compound **2** was prepared by a modified literature procedure.[12] To an acetonitrile solution (100 mL) of 1,4,8,11-tetraazatricyclo[9.3.1.1]hexadecane (**1**) (4.00 g, 178 mmol) was added 2-iodoethyl methyl sulfide (~80% purity, 23.0 g, 91.1 mmol) rapidly. The solution was stirred at room temperature for 48 h. The white precipitate was filtered, washed with acetonitrile, and dried under vacuum to give **2** (8.72 g) in 78% yield. ^{1}H NMR (DMSO-d_6): δ 1.75 (m, 2H, β-CH_2), 2.19 (s, 6H, S−CH_3), 2.36 (m, 4H), 2.64 (d, 2H, J = 14.4 Hz), 2.86−3.10 (m, 8H), 3.16 (t, 2H, J = 14.4 Hz), 3.33−3.35 (m, 4H), 3.46−3.52 (m, 4H), 3.65−3.72 (m, 4H), 4.24 (t, 2H, N−CH_2−N, J = 14.4 Hz), 5.22 (d, 2H, N−CH_2−N, J = 8.9 Hz). ^{13}C{^{1}H} NMR (DMSO-d_6): δ 15.31 (S−CH_3), 19.65 (S−CH_2), 24.75 (β-CH_2), 46.91 (N−CH_2), 47.38 (N−CH_2), 51.43 (α-CH_2), 57.97 (α-CH_2), 59.40 (α-CH_2), 76.79 (N−CH_2−N). Anal. Calcd for $C_{18}H_{38}N_4S_2I_2$: C, 34.40; H, 6.09; N, 8.91; S, 10.20. Found: C, 33.70; H, 5.75; N, 9.01; S, 9.82.

*1,8-Bis(2-[D_3]methythioethyl)-4,11-diazoniatricyclo[9.3.1.1]-hexadecane Diiodide (**2-d_6**).* The deuterated compound **2-d_6** was prepared as described for **2**, but using $CD_3SCH_2CH_2I$ prepared from $CD_3SCH_2CH_2Cl$ accordingly.[39]

1,8-Bis(2-methylthioethyl)-4,11-dimethyl-1,4,8,11-tetraazatetradecane (dmmtc). To a suspension of **2** (2.00 g, 3.18 mmol) in ethanol (50 mL) was added sodium tetrahydroborate (1.20 g, 31.7 mmol) in small portions, and the solution was refluxed for 3 h. After the mixture was cooled to room temperature, aqueous HCl (ca. 3 M, 30 mL) was added slowly, and most of the ethanol was removed by evaporation. The aqueous residue was diluted by water (100 mL) and adjusted to pH > 12 by addition of aqueous NaOH (conc.). The mixture was extracted with chloroform (3 × 100 mL), and the organic phases were collected and dried over $MgSO_4$, and evaporated to dryness to give dmmtc as a sticky white solid in 80% yield, which is sufficiently pure for further use. Recrystallization from hexane gave the analytically pure product. ^{1}H NMR (C_6D_6): δ 1.52 (quint, J = 6.2 Hz, 4H, β-CH_2), 1.87 (s, 6H, S−CH_3), 2.11 (s, 6H, N−CH_3), 2.38 (t, 8H, J = 6.2 Hz, N−CH_2), 2.46−2.50 (m, 8H, N−CH_2+S−CH_2) 2.54 (t, J = 6.9 Hz, 4H, S−CH_2), 2.62−2.63 (m, 4H, N−CH_2). ^{13}C{^{1}H} NMR (C_6D_6): δ 15.52 (S−CH_3), 25.47 (β-CH_2), 32.40 (S−CH_2), 43.31 (N−CH_3), 51.50 (N−CH_2), 52.07 (α-CH_2), 54.84 (α-CH_2), 55.21 (α-CH_2), 55.65 (α-CH_2). ESI-TOF-MS (MeOH): m/z = 377.1 ([M + H]$^+$). Anal. Calcd for $C_{18}H_{40}N_4S_2$: C, 57.40; H, 10.70; N, 14.87; S, 17.03. Found: C, 57.37; H, 10.50; N, 14.91; S, 16.56.

1,8-Bis(2-[D_3]methylthioethyl)-4,11-dimethyl-1,4,8,11-tetraazatetradecane (dmmtc-d_6). Using **2-d_6**, the deuterated ligand dmmtc-d_6 was prepared as described for dmmtc. ESI-TOF-MS (MeOH): m/z = 383.1 ([M + H]$^+$).

1,8-Bis(2-methylthioethyl)-1,4,8,11-tetraazatetradecane (mtc). Compound **2** (2.00 g, 3.18 mmol) was dissolved in an aqueous NaOH solution (3 M, 100 mL), and the solution was refluxed for 1 h. The product was extracted with chloroform (3 × 100 mL), and the organic phases were collected, dried over $MgSO_4$, and evaporated to dryness to give mtc as a sticky white solid in 83% yield, which is sufficiently pure for further use. Recrystallization from hexane gave the analytically pure product. ^{1}H NMR (C_6D_6): δ 1.58 (quint, 4H, β-CH_2), 1.89 (s, 6H, S−CH_3), 2.29 (t, 4H, S−CH_2), 2.37 (m, 4H, N−CH_2), 2.51−2.56 (m, 8H, N−CH_2), 2.61−2.68 (m, 8H, N−CH_2). ^{13}C{^{1}H} NMR (C_6D_6): δ 15.59 (S−-CH_3), 26.94 (β-CH_2), 31.02 (S−CH_2), 48.50 (N−CH_2), 50.82 (N−CH_2), 53.30 (α-CH_2), 53.67 (α-CH_2), 55.16 (α-CH_2). ESI-TOF-MS (MeOH): m/z = 349.1 ([M + H]$^+$). Anal. Calcd for $C_{16}H_{36}N_4S_2$: C, 55.12; H, 10.41; N, 16.07; S, 18.40. Found: C, 55.51; H, 10.12; N, 15.76; S, 18.87.

*[Ni(dmmtc)(Cl)](Cl) (**3**).* To an ethanol solution (20 mL) of dmmtc (1.00 g, 2.65 mmol) was added an aqueous solution (30 mL) of $NiCl_2·6H_2O$ (678 mg, 2.86 mmol), which was stirred at room temperature for 3 h. After the solution was concentrated to ca. 1 mL in vacuo, the green residue was extracted with chloroform (5 × 100 mL), dried over $MgSO_4$, and evaporated to dryness to give **3** as a yellow green powder in 70% yield. Single crystals suitable for X-ray analysis were obtained by recrystallization from CH_2Cl_2/Et_2O. ESI-TOF-MS (CH_3CN): m/z = 469.2 ([M]$^+$). UV−vis (CH_3CN): λ_{max}/nm (ε) = 427 (124), 722 (34). Anal. Calcd for $C_{18}H_{40}N_4S_2NiCl_2$: C, 42.70; H, 7.96; N, 11.07; S, 12.67. Found: C, 42.56; H, 7.55; N, 10.95; S, 12.30.

*[Ni(dmmtc-d_6)(Cl)](Cl) (**3-d_6**).* Complex **3-d_6** was prepared as described for **3** using dmmtc-d_6. ESI-TOF-MS (CH_3CN): m/z = 475.1 ([M]$^+$).

*[Ni(dmmtc)](OTf)$_2$ (**4**).* To an aqueous solution (10 mL) of **3** (1.00 g, 1.98 mmol) was added sodium trifluoromethanesulfonate (1.04 g, 6.04 mmol), and the mixture was stirred at room temperature for 1 h. The blue solution was extracted with nitromethane, and the organic phases were collected, dried over $MgSO_4$, and evaporated to dryness. The bluish-green solid was dissolved in acetonitrile (5 mL), and THF (200 mL) was added. After standing for a day, bluish green crystals of **4** were obtained in 76% yield. ESI-TOF-MS (CH_3CN): m/z (%) = 217.2 ([M]$^{2+}$) (100), 583.1 ([M + OTf]$^+$) (90). UV−vis (CH_3CN): λ_{max}/nm (ε) = 345 (1670), 616 (57). Anal. Calcd for $C_{20}H_{40}N_4S_4F_6NiO_6$: C, 32.75; H, 5.50; N, 7.64; S, 17.49. Found: C, 33.07; H, 5.10; N, 7.67; S, 17.43.

*[Ni(dmmtc-d_6)](OTf)$_2$ (**4-d_6**).* Complex **4-d_6** was prepared as described for **4** from **3-d_6**. ESI-TOF-MS (CH_3CN): m/z (%) = 220.2 ([M]$^{2+}$) (100), 589.1 ([M + OTf]$^+$) (90).

*[Ni(mtc)(Cl)](Cl) (**5a**) and [Ni(mtc)(OH$_2$)$_2$](Cl)$_2$ (**5b**).* To an ethanol solution (20 mL) of mtc (1.40 g, 4.02 mmol) was added an aqueous solution (30 mL) of $NiCl_2·6H_2O$ (1.00 g, 4.21 mmol). This was stirred at room temperature for 3 h. After the mixture was concentrated to 10 mL, a light purple precipitate was collected and washed with ethanol to give **5b** as a purple powder in 16% yield. The filtrate was evaporated to dryness, and the residue was extracted with chloroform, dried over $MgSO_4$, and concentrated to give **5a** as a light blue powder in 63% yield. Single crystals of **5a** and **5b** suited for X-ray analysis were obtained by cooling an CH_3CN/Et_2O solution for **5a** and by slow evaporation of a methanol solution for **5b**. **5a**, ESI-TOF-MS (CH_3CN): m/z = 441.1 ([M]$^+$). UV−vis (CH_3CN): λ_{max}/nm (ε) = 379 (17), 608 (11). Anal. Calcd for $C_{16}H_{36}N_4S_2NiCl_2·C_2H_3N$: C, 41.63; H, 7.57; N, 13.49; S, 12.35. Found: C, 41.67; H, 7.20; N, 13.39; S, 12.80. **5b**, ESI-TOF-MS (CH_3OH): m/z = 441.1 ([M + Cl − 2(H_2O)]$^+$) Anal. Calcd for $C_{16}H_{40}N_4S_2Cl_2NiO_2$: C, 37.37; H, 7.84; N, 10.89; S, 12.47. Found: C, 36.91; H, 7.88; N, 10.74; S, 11.79.

*RRRR-[Ni(mtc)](OTf)$_2$ (**6a**).* To an aqueous solution (10 mL) of *RRRR*-[Ni(mtc)(Cl)](Cl) (**5a**) (480 mg, 1.00 mmol) was added sodium trifluoromethanesulfonate (510 mg, 2.96 mmol), and the mixture was stirred at room temperature for 1 h. The purple solution was extracted with nitromethane, and the organic phases were collected, dried over $MgSO_4$, and concentrated to give **6a** as a violet powder in 88% yield. The crude product was purified by cooling a saturated THF/Et_2O solution to give violet crystals. ESI-TOF-MS (CH_3CN): m/z (%) = 555.2 ([M + OTf]$^+$) (100), 203.1 ([M]$^{2+}$) (30). UV−vis (CH_3CN): λ_{max}/nm (ε) = 352 (26), 554 (17). Anal. Calcd for $C_{18}H_{36}N_4S_4F_6NiO_6$: C, 30.65; H, 5.14; N, 7.94; S, 18.18. Found: C, 31.14; H, 5.27; N, 7.96; S, 17.68.

*RRSS-[Ni(mtc)](OTf)$_2$ (**6b**).* Method A: Complex **6b** was prepared as described for **6a** from **5b** (250 mg, 0.486 mmol) and NaOTf (260 mg, 1.51 mmol) in 91% yield. Method B: To an ethanol solution (50 mL) of nickel(II) triflate hexahydrate (464 mg, 1.00 mmol) was added an ethanol solution (10 mL) of mtc (314 mg, 0.900 mmol), and the orange solution was stirred overnight. Concentration of the solution gave an orange crystalline solid as the first crop of **6b**. The filtrate was evaporated, and the resulting sticky solid was dissolved in THF and after standing for several days gave an orange precipitate. After filtration, the solid was washed with THF and EtOH/THF (1:10) to afford **6b**. The total yield of **6b** was 65%. ESI-TOF-MS (CH_3CN): m/z (%) = 555.2 ([M + OTf]$^+$) (100), 203.1 ([M]$^{2+}$) (30). UV−vis (CH_3CN): λ_{max}/nm (ε) = 285 (2100), 479 (21). Anal. Calcd for $C_{18}H_{36}N_4S_4F_6NiO_6$: C, 30.65; H, 5.14; N, 7.94; S, 18.18. Found: C, 31.05; H, 5.28; N, 7.97; S, 18.29.

dx.doi.org/10.1021/ic300017k | Inorg. Chem. 2012, 51, 5173−5187

*RRRR-[Ni(mtc)](BAr$^F_4$)$_2$ (**7a**).* To a suspension of **6a** (210 mg, 0.298 mmol) in fluorobenzene (10 mL) was added NaBAr$^F_4$ (536 mg, 0.605 mmol), and the mixture was stirred at room temperature for 1 h. After the precipitates were filtered off, the filtrate was evaporated and washed with Et_2O/hexane (1:1) to give **7a** as a light purple powder in 90% yield. UV−vis (THF): λ_{max}/nm (ε) = 550 (22). Anal. Calcd for $C_{80}H_{60}N_4S_2B_2F_{48}Ni$: C, 45.03; H, 2.83; N, 2.63; S, 3.01. Found: C, 45.07; H, 2.91; N, 2.63; S, 2.71.

*RRSS-[Ni(mtc)](BAr$^F_4$)$_2$ (**7b**).* To a solution of **6b** (315 mg, 0.447 mmol) in MeOH/CH_3CN (a 2:1 mixture, 10 mL) was added NaBAr$^F_4$ (720 mg, 0.812 mmol), and this was stirred at room temperature for 1 h. The mixture was evaporated to dryness and washed with water to give **7b** as a light purple powder in 74% yield. Single crystals suitable for X-ray analysis were grown by cooling a saturated THF/Et_2O solution. UV−vis (THF): λ_{max}/nm (ε) = 476 (15). Anal. Calcd for $C_{80}H_{60}N_4S_2B_2F_{48}Ni$: C, 45.03; H, 2.83; N, 2.63; S, 3.01. Found: C, 45.41; H, 2.86; N, 3.01; S, 2.70.

*[Ni(dmmtc)](OTf) (**8**).* Complex **4** (1.00 g, 1.36 mmol) was dissolved in a THF/CH_3CN (a 5:1 mixture, 10 mL), and 0.3% Na/Hg (50 g) was added. After the mixture was stirred for 20 min, ether was added to the green solution to afford a light blue powder. The product was dissolved into fluorobenzene, and the insoluble NaOTf was filtered off. Slow addition of ether to the filtrate afforded **8** as light blue crystals in 72% yield. ESI-TOF-MS (THF): m/z = 434.2 ([M]$^+$). UV−vis (THF): λ_{max}/nm (ε) = 333 (3600), 717 (20). Anal. Calcd for $C_{19}H_{40}N_4S_3F_3NiO_3$: C, 39.05; H, 6.90; N, 9.59; S, 16.46. Found: C, 39.42; H, 6.71; N, 9.65; S, 16.04. EPR spectrum was recorded at 8 K for a finely grinded crystalline light blue powder.

*[Ni(dmmtc-d_6)](OTf) (**8-d_6**).* Complex **8-d_6** was prepared from **4-d_6** as described for **8**. ESI-TOF-MS (THF): m/z = 440.2 ([M]$^+$).

*[Ni(dmmtc)](BAr$^F_4$) (**9**).* To a suspension of **8** (116 mg, 0.198 mmol) in ether (10 mL) was added NaBAr$^F_4$ (178 mg, 0.201 mmol), and this was stirred at room temperature for 1 h. After filtration, vapor diffusion of pentane into the filtrate at −40 °C resulted in the formation of yellow crystals of **9** in 70% yield. ESI-TOF-MS (THF): m/z = 434.2 ([M]$^+$). Anal. Calcd for $C_{50}H_{52}N_4S_2BF_{24}Ni$: C, 46.25; H, 4.04; N, 4.31; S, 4.94. Found: C, 46.56; H, 4.06; N, 4.29; S, 4.45. EPR spectrum was recorded at 8 K for a finely grinded crystalline yellow powder.

*RSRS-[Ni(mtc)](BAr$^F_4$) (**10a**).* During this procedure, the temperature was kept below −40 °C. Complex **7b** (200 mg, 0.0937 mmol) was dissolved in THF/ether (a 1:10 mixture, 2 mL), and 0.3% Na/Hg (10 g) was added. After being stirred for 20 min, the mixture was filtered, and pentane was added slowly to the filtrate to give **10a** as a green precipitate. Vapor diffusion of pentane into a solution of **10a** in THF/Et_2O (a 1:20 mixture, 1 mL) afforded **10a** as yellow green crystals in 51% yield. **10a**; UV−vis (THF): λ_{max}/nm (ε) = 335 (3100). Anal. Calcd for $C_{48}H_{48}N_4S_2BF_{24}Ni$: C, 45.38; H, 3.81; N, 4.41; S, 5.05. Found: C, 45.26; H, 3.59; N, 4.11; S, 5.05. EPR spectrum was recorded at 190 K for a finely grinded crystalline green powder.

A small amount of **10b** was obtained as yellow crystals together with **10a** when pentane was quickly added to the filtrate after the same reduction, and the structure was characterized by X-ray analysis.

GC Analysis of the Gaseous Products. The various Ni(I) complexes were allowed to react in a Schlenk tube with a Young valve, and the gaseous products were analyzed with a Shimadzu GC-8A gas chromatograph equipped with TCD detector and integrator Shimadzu CR-6A, using a 2 m long packed column SHINCARBON-ST. Measurement conditions: CH_4; injector temperature = 120 °C, detector temperature = 120 °C, column temperature = 60 °C, flow 50 mL/min. C_2H_4 and C_2H_6; injector temperature = 180 °C, detector temperature = 180 °C, column temperature = 150 °C, flow 50 mL/min. The products were identified by comparison of their retention times with those of authentic standard compounds. Their yields were determined from the areas of the corresponding eluted peaks using calibration curves. The deuterated products, CD_3H and C_2D_6, were determined by GC−MS Shimadzu GCMS-QP2010 with a 30 m long Rt-Qplot column under isothermal conditions at 40 °C.

*Reaction of **8**.* In a 200 mL Schlenk tube with a Young valve was dissolved the Ni(I) complex **8** (120 mg, 0.206 mmol) in THF (5 mL), and then it was stirred at 75 °C for 4 d. After being cooled to room temperature, both the solution and the headspace-gas of the Schlenk tube were analyzed by GC, which shows the yields of methane, ethane, and ethylene as 6%, 23%, and 3%, respectively, as a sum of those in the solution and gas phases. The solution was filtered to give the crystalline solids **4** and **4′**. The blue green crystals of **4** and light blue crystals of **4′** were isolated in ∼2% yield by selecting the crystals under a microscope. The filtrate was evaporated and washed by THF/Et_2O to remove the remaining small amount of **8**. The residue was dissolved in THF and concentrated to give brownish green crystals of **12** in 19% yield. **12**, ESI-TOF-MS (THF): m/z = 419.2 ([M]$^+$). UV−vis (THF): λ_{max}/nm (ε) = 377 (1600), 712 (21). Anal. Calcd for $C_{18}H_{37}N_4S_3F_3NiO_3$: C, 37.97; H, 6.55; N, 9.84; S, 16.89. Found: C, 38.13; H, 6.62; N, 9.81; S, 16.49. **4′**: ESI-TOF-MS (CH_3CN), m/z = 217.1 ([M]$^{2+}$). Anal. Calcd for $C_{20}H_{40}N_4S_4F_6NiO_6$: C, 32.75; H, 5.50; N, 7.64; S, 17.49. Found: C, 32.83; H, 5.60; N, 7.60; S, 17.08.

*Reaction of **8** with DmpSH.* In a 200 mL Schlenk tube with a Young valve were dissolved complex **8** (120 mg, 0.205 mmol) and DmpSH (345 mg, 1.00 mmol) in THF (5 mL), and then they were stirred at 75 °C for 4 d. After being cooled to room temperature, both the solution and the headspace-gas of the Schlenk tube were analyzed by GC, which shows the yields of methane and ethylene as 31% and 3%, respectively, as a sum of those in the solution and gas phases. The solution was filtered to give a small amount of **4** and **4′** as crystalline solids. The filtrate was evaporated, and the residue was first extracted with ether, evaporated, and separated by HPLC to give $DmpSCH_3$ in 12% yield. The ether insoluble residue was extracted with THF and concentrated to give **12** as yellow green crystals in 21% yield.

Synthesis of $DmpSCH_3$. To a THF solution (50 mL) of DmpSH (345 mg, 1.00 mmol) was added *n*-butyllithium (1.6 M in hexane, 0.66 mL, 1.05 mmol) at −20 °C, and the mixture was stirred at room temperature for 30 min. Iodomethane (0.10 mL, 1.6 mmol) was added to the solution and stirred for 1 h. After evaporation, the residue was dissolved in CH_2Cl_2. The organic layer was washed with water (100 mL), dried over $MgSO_4$, and evaporated to dryness to give $DmpSCH_3$ as a white powder in 80% yield. ^{1}H NMR ($CDCl_3$): δ 1.71 (s, 3H, SCH_3), 2.04 (s, 12H, *o*-CH_3 of Mes), 2.33 (s, 6H, *p*-CH_3 of Mes), 6.95 (s, 4H, *m*-CH of Mes), 7.06 (d, J = 7.6 Hz, 2H, *m*-CH of Dmp), 7.36 (t, J = 7.6 Hz, 1H, *p*-CH of Dmp). Anal. Calcd for $C_{25}H_{28}S$: C, 83.28; H, 7.83; S, 8.89. Found: C, 83.11; H, 7.42; S, 8.30.

*Reaction of **11**.* [Ni(mtc)]OTf (**11**) was prepared by treatment of **6a** (140 mg, 0.198 mmol) with 0.3% Na/Hg (10 g) in THF (3 mL) at −40 °C followed by filtration. The THF solution of **11** was warmed to room temperature and stirred at for 6 h. Both the solution and the headspace-gas of the Schlenk tube were analyzed by GC, which shows the yields of methane and ethylene were 30% and 2%, respectively, as a sum of those in the solution and gas phases. The solution was evaporated and extracted with fluorobenzene. After slow addition of ether, the solution stood for a day to give deep blue crystals of **18** (5% yield) with a small amount of green crystals of **17**. After the solution was evaporated to dryness, the solid was dissolved in fluorobenzene (1 mL). Vapor diffusion of pentane afforded **17** as green crystals in 9% yield. **17**, ESI-TOF-MS (THF): m/z = 391.0 ([M]$^+$). UV−vis (THF): λ_{max}/nm (ε) = 405 (160). Anal. Calcd for $C_{16}H_{33}N_4S_3F_3NiO_3{\cdot}C_3H_{2.5}F_{0.}$: C, 38.72; H, 6.07; N, 9.51; S, 16.32. Found: C, 38.82; H, 6.53; N, 9.63; S, 15.96. **18**, ESI-TOF-MS (THF): m/z = 405.1 ([M]$^+$). UV−vis (THF): λ_{max}/nm (ε) = 357 (1200). Anal. Calcd for $C_{17}H_{35}N_4S_3F_3NiO_3{\cdot}C_3H_{2.5}F_{0.5}$: C, 39.81; H, 6.26; N, 9.28; S, 15.94. Found: C, 39.72; H, 6.03; N, 9.66; S, 15.78.

X-ray Structural Determination. Crystal data and refinement parameters for the structurally characterized complexes are summarized in Table 8. Single crystals were coated with oil (CryoLoop, Immersion Oil, Type B or Paraton, Hampton Research Corp.) and mounted on loops. Diffraction data were collected on a Rigaku AFC-8 instrument equipped with a Mercury CCD detector (for **5a**, **6a**, **6b**, **8**, **10b**, **12**, **17**) or with a Saturn 70 CCD detector (for **4**, **18**, *RSRS*-[Ni(tmc)]OTf) or Rigaku AFC-10 instrument equipped with a Saturn 70 CCD detector (for **3**, **4′**, **5b**, **7b**, **9**, **10a**). The measurements were made by using graphite-monochromized Mo Kα radiation (λ = 0.71070 Å) under a cold nitrogen stream. The frame data were integrated and

dx.doi.org/10.1021/ic300017k | *Inorg. Chem.* 2012, 51, 5173−5187

Table 8. Crystal Data for 3, 4, 4′, 5a,b, 6a,b, 7b, 8, 9, 10a,b, 12, 17, 18, and *RSRS*-[Ni(tmc)]OTf

	complex					
	3	**4**	**4′**	**5a**·CH_3CN	**5b**	**6a**
formula	$C_{18}H_{40}Cl_2N_4NiS_2$	$C_{20}H_{40}F_6N_4NiO_6S_4$	$C_{20}H_{40}N_4F_6NiO_6S_4$	$C_{18}H_{39}N_5Cl_2NiS_2$	$C_{16}H_{40}N_4Cl_2NiS_2O_2$	$C_{18}H_{36}N_4F_6NiO_6S_4$
formula wt	506.27	733.49	733.49	519.27	514.24	705.44
crystal system	monoclinic	monoclinic	monoclinic	triclinic	triclinic	monoclinic
space group	$P2_1/c$ (No. 14)	$P2_1/c$ (No. 14)	$P2_1/n$ (No. 14)	$P\bar{1}$ (No. 2)	$P\bar{1}$ (No. 2)	$P2_1/c$ (No. 14)
a, Å	9.501(4)	9.7762(14)	10.024(2)	8.4501(11)	7.5090(18)	12.662(3)
b, Å	11.257(5)	16.381(2)	13.095(3)	9.3231(12)	8.642(2)	16.384(3)
c, Å	22.727(10)	18.872(3)	11.323(3)	16.278(2)	9.741(2)	13.884(3)
α, deg	90	90	90	76.105(4)	99.0400(15)	90
β, deg	94.519(10)	90.572(2)	94.634(3)	78.074(5)	97.791(4)	91.787(2)
γ, deg	90	90	90	83.894(5)	109.709(3)	90
V, Å^3	2423.0(19)	3022.1(8)	1481.5(6)	1215.8(3)	575.5(2)	2878.9(11)
Z	4	4	2	2	1	4
ρ_{calcd}, g cm^{-1}	1.388	1.612	1.644	1.418	1.484	1.627
μ, cm^{-1}	12.049	9.973	10.171	12.038	12.756	10.433
F_{000}	1080	1528	764	552	274	1464
$2\theta_{max}$, deg	55.0	54.9	55.0	55.0	54.9	55.0
no. of rflns collected	19 141	24 146	17 367	14 433	6919	33 548
indep (R_{int})	5408 (0.067)	6894 (0.028)	3380 (0.097)	5528 (0.028)	2598 (0.144)	6572 (0.0379)
no. of params	245	371	188	254	125	336
R1[a]	0.0585	0.0445	0.0638	0.0317	0.0525	0.0712
wR2[b]	0.1545	0.1085	0.1570	0.0775	0.1632	0.2013
GOF on F^2[c]	1.079	1.006	1.059	1.047	1.045	1.080
CCDC	860248	860249	860250	860251	860252	860253

	6b	**7b**·4THF	**8**	**9**·Et_2O	**10a**·THF	**10b**·THF·Et_2O	**12**
formula	$C_{18}H_{36}N_4F_6NiO_6S_4$	$C_{96}H_{92}N_4B_2F_{48}NiO_4S_2$	$C_{19}H_{40}N_4F_3NiO_3S_3$	$C_{54}H_{62}N_4BF_{24}NiOS_2$	$C_{52}H_{56}N_4BF_{24}NiOS_2$	$C_{56}H_{66}N_4BF_{24}NiO_2S_2$	$C_{18}H_{37}N_4F_3NiO_3S_3$
formula wt	705.44	2422.17	584.43	1372.70	1342.63	1416.75	569.39
crystal system	triclinic	triclinic	monoclinic	triclinic	triclinic	triclinic	monoclinic
space group	$P\bar{1}$ (No. 2)	$P\bar{1}$ (No. 2)	$C2/c$ (No. 15)	$P\bar{1}$ (No. 2)	$P\bar{1}$ (No. 2)	$P\bar{1}$ (No. 2)	$P2_1/c$ (No. 14)
a, Å	9.066(2)	12.3465(15)	29.540(9)	12.9215(13)	12.315(4)	13.181(5)	9.907(2)
b, Å	9.318(3)	13.3250(15)	9.348(3)	12.9799(13)	13.054(4)	13.247(5)	13.538(3)
c, Å	9.914(3)	17.4185(18)	20.501(6)	19.3935(19)	18.427(6)	20.337(7)	18.939(5)
α, deg	72.573(15)	71.676(5)	90	99.7353(8)	89.158(9)	97.060(3)	90
β, deg	70.020(15)	70.960(4)	110.247(4)	100.0680(14)	87.784(8)	107.688(5)	99.500(3)
γ, deg	63.973(13)	86.426(6)	90	100.6688(18)	86.825(9)	103.838(4)	90
V, Å^3	696.1(3)	2568.9(5)	5311(3)	3078.3(5)	2955(2)	3211(2)	2505.2(10)
Z	1	1	8	2	2	2	4
ρ_{calcd}, g cm^{-1}	1.683	1.566	1.462	1.481	1.509	1.465	1.510
μ, cm^{-1}	10.788	3.692	10.152	4.967	4.813	4.799	10.740
F_{000}	366	1230	2472	1406	1370	1454	1200
$2\theta_{max}$, deg	55.0	55.0	55.0	54.9	55.0	55.0	55.0

dx.doi.org/10.1021/ic300017k | *Inorg. Chem.* 2012, 51, 5173−5187

Table 8. continued

	6b	7b·4THF	8	9·Et_2O	10a·THF	10b·THF·Et_2O	12
no. of rflns							
collected	8283	31 408	20 070	36 815	24 014	38 218	19 461
indep (R_{int})	3172 (0.032)	11 685 (0.080)	5977 (0.0597)	13 930 (0.045)	8369 (0.0552)	14 650 (0.0755)	5724 (0.041)
no. of params	179	734	505	777	789	949	290
R1[a]	0.0422	0.0807	0.0899	0.0735	0.1006	0.0759	0.0660
wR2[b]	0.1068	0.2392	0.3137	0.2116	0.2711	0.2386	0.1814
GOF on F^2[c]	1.051	1.056	1.184	1.043	1.093	1.033	1.040
CCDC	860254	860255	860256	860257	860258	860259	860290

	17·0.5(C_6H_5F)	18·0.5(C_6H_5F)	*RSRS*-[Ni(tmc)]OTf
formula	$C_{19}H_{35.5}N_4F_{3.5}NiO_3S_3$	$C_{20}H_{37.5}N_4F_{3.5}NiO_3S_3$	$C_{15}H_{32}N_4F_3NiO_3S$
formula wt	589.39	603.42	464.20
crystal system	triclinic	triclinic	orthorhombic
space group	$P\bar{1}$ (No. 2)	$P\bar{1}$ (No. 2)	*Pna*2 (No. 33)
a, Å	10.048(2)	8.6154(14)	18.709(3)
b, Å	11.535(2)	12.5521(15)	11.982(2)
c, Å	11.579(2)	14.1876817)	9.4404(17)
α, deg	75.968(5)	113.522(7)	90
β, deg	88.639(5)	101.034(8)	90
γ, deg	83.670(5)	98.780(10)	90
V, Å^3	1294.0(4)	1335.3(3)	2116.2(7)
Z	2	2	4
ρ_{calcd}, g cm^{-1}	1.513	1.501	1.457
μ, cm^{-1}	10.452	10.148	10.633
F_{000}	618	634	980
$2\theta_{max}$, deg	54.9	55.0	55.0
no. of rflns			
collected	15 356	16 349	15 972
indep (R_{int})	5882 (0.024)	6081 (0.035)	3989 (0.022)
no. of params	308	317	245
R1[a]	0.0376	0.0332	0.0269
wR2[b]	0.960	0.0806	0.0741
GOF on F^2[c]	1.038	1.026	1.041
CCDC	860261	860262	860263

[a] $R1 = \sum_{||}F_o| - |F_{c||}/\sum|F_o|$ ($I > 2\sigma(I)$). [b] $wR2 = [(\sum w(|F_o| - |F_c|)^2/\sum wF_o^2)]^{1/2}$ (all data). [c] $GOF = [\sum w(|F_o| - |F_c|)^2/(N_o - N_v)]^{1/2}$ (N_o = number of observations, N_v = number of variables).

dx.doi.org/10.1021/ic300017k | *Inorg. Chem.* 2012, 51, 5173−5187

corrected for absorption with the Rigaku/MSC CrystalClear program package. The structures were solved with use of direct methods (SIR-92 or SIR-97) and standard difference map techniques and were refined by full-matrix least-squares procedures on F^2 using the Rigaku/MSC CrystalStructure package. Anisotropic refinement was applied to all non-hydrogen atoms except for the disordered atoms that include a dmmtc ligand for **8**, a $CH_3SCH_2CH_2$ chain for **10a**, a triflate anion for **6a**, trifluoromethyl groups of $BAr^F{}_4^-$, and the crystalline solvent THF for **10a** and fluorobenzene for **17** and **18**, in which the ratios were refined freely while the total occupancy of the components was constrained to unity (see the Supporting Information). All of the hydrogen atoms were placed at calculated positions. Additional crystallographic data are given in the Supporting Information.

■ ASSOCIATED CONTENT

Supporting Information

Crystallographic data in CIF format for **3**, **4**, **4′**, **5a,b**, **6a,b**, **7b**, **8**, **9**, **10a,b**, **12**, **17**, **18**, *RSRS*-[Ni(tmc)]OTf, synthesis of *RSRS*-[Ni(tmc)](OTf) and [Ni(tmc)]($BAr^F{}_4$), molecular structures and metric parameters of **3**, *RSRS*-[Ni(tmc)](OTf), and **4′**, CV data for **8**, and EPR spectrum of [Ni(tmc)]($BAr^F{}_4$). This material is available free of charge via the Internet at http://pubs.acs.org.

■ AUTHOR INFORMATION

Corresponding Author

*E-mail: i45100a@nucc.cc.nagoya-u.ac.jp.

Notes

The authors declare no competing financial interest.

■ ACKNOWLEDGMENTS

This research was financially supported by Grant-in-Aids for Scientific Research (nos. 18GS0207 and 23000007) from the Ministry of Education, Culture, Sports, Science, and Technology, Japan. We thank Prof. Tatsuhisa Kato (Kyoto University) for fruitful discussions on EPR spectra. We are grateful to Prof. Roger E. Cramer for discussions and careful reading of the manuscript.

■ REFERENCES

(1) (a) Grabarse, W.; Shima, S.; Mahlert, F.; Duin, E. C.; Thauer, R. K.; Ermler, U. In *Handbook of Metalloproteins*; Messershmidt, A., Huber, R., Poulos, T., Wieghardt, K., Eds.; John Wiley & Sons: New York, 2001; Vol. 2, pp 897−914. (b) DiMarco, A. A.; Bobik, T. A.; Wolfe, R. S. *Annu. Rev. Biochem.* **1990**, *59*, 355−394. (c) Gunsalus, R. P.; Wolfe, R. S. *FEMS Microbiol. Lett.* **1978**, *3*, 191−193. (d) Ellefson, W. L.; Whitman, W. B.; Wolfe, R. S. *Proc. Natl. Acad. Sci. U.S.A.* **1982**, *79*, 3707−3710. (e) Pfaltz, A.; Livingston, D. A.; Juan, B.; Diekert, G.; Thauer, R. K.; Eschenmoser, A. *Helv. Chim. Acta* **1985**, *68*, 1338−1358. (f) Halcrow, M. A.; Christou, G. *Chem. Rev.* **1994**, *94*, 2421−2481. (g) Thauer, R. K. *Microbiology* **1998**, *144*, 2377−2406.

(2) (a) Grabarse, W.; Mahlert, F.; Shima, S.; Thauer, R. K.; Ermler, U. *J. Mol. Biol.* **2000**, *303*, 329−344. (b) Grabarse, W.; Shima, S.; Goubeaud, M.; Thauer, R. K. *Science* **1997**, *278*, 1457−1462. (c) Grabarse, W.; Mahlert, F.; Duin, E. C.; Goubeaud, M.; Shima, S.; Thauer, R. K.; Lamzin, V.; Ermler, U. *J. Mol. Biol.* **2001**, *309*, 315−330.

(3) (a) Jaun, B. In *Metal Ions in Life Science*; Sigel, A., Sigel, H., Sigel, R. K. O., Eds.; John Wiley & Sons: Chichester, UK, 2007; Vol. 2, pp 323−356. (b) Albracht, S. P. J.; Ankel-Fuchs, D.; Bocher, R.; Ellennann, J.; Moll, J.; van der Zwaan, J. W.; Thauer, R. K. *Biochim. Biophys. Acta* **1988**, *955*, 86−102. (c) Albracht, S. P. J.; Ankel-Fuchs, D.; van der Zwaan, J. W.; Fontjin, R. D.; Thauer, R. K. *Biochim. Biophys. Acta* **1986**, *870*, 50−57. (d) Ermler, U. *Dalton Trans.* **2005**, 3451−3458. (e) Färber, G.; Keller, W.; Kratky, C.; Jaun, B.; Pfaltz, A.; Spinner, C.; Kobelt, A.; Eschenmoser, A. *Helv. Chim. Acta* **1991**, *74*, 697−716. (f) Pfaltz, A.; Jaun, B.; Fässler, A.; Eschenmoser, A.; Jaenchen, R.; Gilles, H. H.; Diekert, G.; Thauer, R. K. *Helv. Chim. Acta* **1982**, *65*, 828−865.

(4) (a) Rospert, S.; Böcher, R.; Albracht, S. P. J.; Thauer, R. K. *FEBS Lett.* **1991**, *291*, 371−375. (b) Goubeaud, M.; Schreiner, G.; Thauer, R. K. *Eur. J. Biochem.* **1997**, *243*, 110−114. (c) Telser, J.; Davydov, R.; Horng, Y.-C.; Ragsdale, S. W.; Hoffman, B. M. *J. Am. Chem. Soc.* **2001**, *123*, 5853−5860. (d) Duin, E. C.; Piskorski, R.; Mahlert, F.; Clay, M. D.; Goenrich, M.; Thauer, R. K.; Jaun, B. *J. Biol. Inorg. Chem.* **2004**, *9*, 563−574. (e) Mahlert, F.; Bauer, C.; Jaun, B.; Thauer, R. K.; Duin, E. C. *J. Biol. Inorg. Chem.* **2002**, *7*, 500−513.

(5) (a) Zilbermann, I.; Golub, G.; Cohen, H.; Meyerstein, D. *Inorg. Chim. Acta* **1994**, *227*, 1−3. (b) Signor, L.; Knuppe, C.; Hug, R.; Schweizer, B.; Pfaltz, A.; Jaun, B. *Chem.-Eur. J.* **2000**, *6*, 3508−3516. (c) Ram, M. S.; Riordan, C. G.; Ostrander, R.; Rheingold, A. L. *Inorg. Chem.* **1995**, *34*, 5884−5892.

(6) (a) Pelmenschikov, V.; Blomberg, M. R. A.; Siegbahn, Per E. M.; Crabtree, R. H. *J. Am. Chem. Soc.* **2002**, *124*, 4039−4049. (b) Pelmenschikov, V.; Siegbahn, Per E. M. *J. Biol. Inorg. Chem.* **2003**, *8*, 653−662.

(7) (a) Lin, S.-K.; Jaun, B. *Helv. Chim. Acta* **1992**, *75*, 1478−1490. (b) Jaun, B.; Pfaltz, A. *J. Chem. Soc., Chem. Commun.* **1986**, 293−296.

(8) A five-coordinated Ni(I) azamacrocyclic complex was reported, see: Suh, M. P.; Oh, K. Y.; Lee, J. W.; Bae, Y. Y. *J. Am. Chem. Soc.* **1996**, *118*, 777−783.

(9) The Ni(I) azamacrocyclic complexes have been reported, see: (a) Szalda, D. J.; Fujita, E.; Sanzenbacher, R.; Paulus, H.; Elias, H. *Inorg. Chem.* **1994**, *33*, 5855−5863. (b) Suh, M. P.; Kim, H. K.; Kim, M. J.; Oh, K. Y. *Inorg. Chem.* **1992**, 3620−3625. (c) Furenlid, L. R.; Renner, M. W.; Szalda, D. J.; Fujita, E. *J. Am. Chem. Soc.* **1991**, *113*, 883−892.

(10) (a) Nishigaki, J.; Matsumoto, T.; Tatsumi, K. *Eur. J. Inorg. Chem.* **2010**, 5011−5017. (b) Nishigaki, J.; Matsumoto, T.; Tatsumi, K. *Inorg. Chem.* **2012**, *51*, 3690−3697.

(11) Previously, Kaden and co-workers synthesized the nickel(II) complexes having similar cyclam derivatives with appended CH_3−S group and investigated their redox properties by CV, see: (a) Schmid, C. L.; Kempf, C.; Taubert, A.; Neuburger, M.; Zehnder, M.; Kaden, T. A. *Helv. Chim. Acta* **1996**, *79*, 1011−1020. (b) Schmid, C.; Neuburger, M.; Zehnder, M.; Kaden, T. A. *Helv. Chim. Acta* **1997**, *80*, 241−252.

(12) Royal, G.; Dahaoui-Gindrey, V.; Dahaoui, S.; Tabart, A.; Guilard, R.; Pullumbi, P.; Lecomte, C. *Eur. J. Org. Chem.* **1998**, 1971−1975.

(13) See Supporting Information, Figure S1 for the X-ray structural analysis of **3**.

(14) The notation of conformation of tetra- or di-*N*-substituted cyclam takes over that of common cyclam metal complexes, which is determined by the chirality on the nitrogen atoms. See: Bosnich, B.; Poon, C. K.; Tobe, M. L. *Inorg. Chem.* **1965**, *4*, 1102−1108.

(15) (a) Vetrichelvan, M.; Lai, Y.-H.; Mok, K. F. *Eur. J. Inorg. Chem.* **2004**, *10*, 2086−2095. (b) Ciampolini, M.; Nardi, N.; Dapporto, P.; Zanobini, F. *J. Chem. Soc., Dalton Trans.* **1984**, 995−998. (c) Blake, A. J.; Halcrow, M. A.; Schroder, M. *J. Chem. Soc., Dalton Trans.* **1992**, 2803−2808. (d) Blake, A. J.; Gould, R. O.; Halcrow, M. A.; Schroder, M. *J. Chem. Soc., Dalton Trans.* **1993**, 2909−2920.

(16) The redox potential of F_{430} pentamethyl ester (F_{430M}) was reported by B. Jaun (see ref 17) and was estimated as −1.49 V using the Ag/Ag^+ potential vs Fc/Fc^+ in acetonitrile.[18]

(17) Piskorski, R.; Jaun, B. *J. Am. Chem. Soc.* **2003**, *125*, 13120−13125.

(18) Connelly, N. G.; Geiger, W. E. *Chem. Rev.* **1996**, *96*, 877−910.

(19) The relative stereochemistry of the mtc ligands of **5a** and **5b** can be described as *cis*-V (*RRRR*) and *trans*-III (*RRSS*) configurations, respectively; see ref 14.

(20) A similar solvent molecule dissociation from Ni(II) cyclam complexes has been reported, see: Boiocchi, M.; Fabbrizzi, L.; Foti, F.; Vázquwz, M. *Dalton Trans.* **2004**, 2616−2620.

(21) The Ni^{I}/Ni^{II} redox potential of $[Ni^{I}(dmmtc)](OTf)$ (**8**) in THF was observed at −0.93 V vs $Ag/AgNO_3$. See Supporting Information, Figure S4.
(22) Fox, D. C.; Fiedler, A. T.; Halfen, H. L.; Brunold, T. C.; Halfen, J. A. *J. Am. Chem. Soc.* **2004**, *126*, 7627−7636.
(23) Ram, M. S.; Babac, A.; Espenson, J. H. *Inorg. Chem.* **1988**, *27*, 4231−4235.
(24) The ORTEP drawing and crystallographic data of *RSRS*-[Ni(tmc)](OTf) were shown in Supporting Information, Figure S2 and Table S3.
(25) The crystal of **10b** contains two half molecules in an asymmetric unit, and the other halves are generated by symmetry operation. One of the two independent molecule structure is shown in Figure 9, and its metric parameters are included in Table 3, because the two structures are very much alike.
(26) Bondi, A. *J. Phys. Chem.* **1964**, *68*, 441−451.
(27) See Supporting Information, Figure S5.
(28) Beley, M.; Collin, J.-P.; Ruppert, R.; Sauvage, J.-P. *J. Am. Chem. Soc.* **1986**, *108*, 7461−7467.
(29) The yields were calculated on the basis of nickel.
(30) The product yields were calculated from the amount of the isolated crystalline materials, and thus the values are underestimated. The ESI-TOF-MS indicated that the isolated nickel complexes are the major products, although a slight amount of insoluble black precipitates was found in the resultant solutions after the reactions.
(31) The structure of **4′** was determined by X-ray diffraction; see the Supporting Information.
(32) Tada, M.; Masuzawa, Y. *Chem. Commun.* **1997**, 2161−2162.
(33) $[Ni(dmmtc)(STol)]^{+}$ was observed in ESI mass spectra. A similar reaction was reported that $[Ni^{I}(tmc)]OTf$ reacted with organic thiols to form $[Ni^{II}(tmc)(SR)]OTf$ with hydrogen emittion. See ref 7.
(34) Ellison, J. J.; Rhulandt-Senge, K.; Power, P. P. *Angew. Chem., Int. Ed. Engl.* **1994**, *33*, 1178−1180.
(35) The yield of $DmpSCH_3$ was calculated from ^{1}H NMR spectra.
(36) A related Ni(II) thiolate was reported, see: Halfen, J. A.; Young, V. G., Jr. *Chem. Commun.* **2003**, 2894−2895.
(37) Homolysis of methylhalide was previously reported, see: (a) Ram, R. S.; Bakac, A.; Espenson, J. M. *Inorg. Chem.* **1986**, *25*, 3267−3272. (b) Bakac, A.; Espenson, J. H. *J. Am. Chem. Soc.* **1986**, *108*, 713−719.
(38) D'Aniello, M. J. Jr.; Barefield, E. K. *J. Am. Chem. Soc.* **1976**, *98*, 1610−1612.
(39) Sunko, D. E.; Branko, J.; Mladen, L. *J. Org. Chem.* **1987**, *52*, 2299.